

Research Paper

Cite this article: Amin OM, Heckmann RA, Dallarés S, Constenla M, Rubini S (2020). Description and molecular analysis of an Italian population of *Centrorhynchus globocaudatus* (Zeder, 1800) Lühe, 1911 (Acanthocephala: Centrorhynchidae) from *Falco tinnunculus* (Falconidae) and *Buteo buteo* (Accipitridae). *Journal of Helminthology* **94**, e207, 1–21. <https://doi.org/10.1017/S0022149X20000887>

Received: 6 August 2020

Accepted: 22 September 2020

Key words:

Acanthocephala; *Centrorhynchus globocaudatus*; redescription; Italy; *Falco*; *Buteo*; new features; molecular profile

Author for correspondence:

O.M. Amin, E-mail: omaramin@aol.com

Description and molecular analysis of an Italian population of *Centrorhynchus globocaudatus* (Zeder, 1800) Lühe, 1911 (Acanthocephala: Centrorhynchidae) from *Falco tinnunculus* (Falconidae) and *Buteo buteo* (Accipitridae)

O.M. Amin¹ , R.A. Heckmann², S. Dallarés³, M. Constenla³ and S. Rubini⁴

¹Institute of Parasitic Diseases, 11445 E Via Linda 2-419, Scottsdale, Arizona 85259, USA; ²Department of Biology, Brigham Young University, 1114 MLBM, Provo, Utah 84602, USA; ³Department of Animal Biology, Vegetal Biology and Ecology, Universitat Autònoma de Barcelona, Cerdanyola, 08193 Barcelona, Spain and ⁴Experimental Zooprophyllactic Institute of Ferrara, St Modena 483, 44124 Cassana, Ferrara, Italy

Abstract

Centrorhynchus globocaudatus (Zeder, 1800) Lühe, 1911 (Centrorhynchidae) was reported in birds of prey. Our population from *Falco tinnunculus* Linnaeus (Falconidae) and *Buteo buteo* Linnaeus (Accipitridae) in northern Italy was morphologically distinct from others described elsewhere. The worms are elongate and cylindrical. Proboscis long, apically truncated and bare, with wider base and variably faint constriction at point of attachment of receptacle. Large anterior hooks well rooted; posterior spiniform hooks with reduced roots; transitional hooks with scutiform roots in-between. Four tubular cement glands extend into prominent ducts overlapping a large Saefftigen's pouch. Bursa large, with sensory plates. Vagina with laterally slit orifice in sub-ventral pit of globular terminal extension. Thick-shelled eggs ovoid without polar prolongation of fertilization membrane. In our specimens, proboscis hooks, receptacle, male reproductive system, and lemnisci especially in males varied in size from those from Ukraine, India, Egypt, Kyrgystan, Russia, Georgia, Armenia and Asian Soviet Republics. Our description of the Italian specimens includes new morphological information supported by scanning electron microscopy and microscope images, molecular analysis and energy dispersive X-ray analysis (EDXA) of hooks. Additional new details of proboscis hook roots, micropores and micropore distribution are described. Metal composition of hooks (EDXA) demonstrated high levels of calcium and phosphorous, and high levels of sulphur in core and cortical layers of eggs. The molecular profile based on sequences of 18S and cytochrome *c* oxidase 1 genes is also provided, as well as phylogenetic reconstructions including all available sequences of the family Centrorhynchidae, although further sequences are needed in order to clarify their phylogenetic relationships.

Introduction

Golvan erected *Sphaerirostris* Golvan, 1956 as a subgenus of *Centrorhynchus* Lühe, 1911 and included 21 species with short spindle-shaped trunk, polydendritic lacunar system, three or four tubular cement glands and short globular anterior proboscis. *Centrorhynchus*, on the other hand, has long and cylindrical trunk with anterior dilation, transverse anastomoses of secondary lacunar vessels, 3–4 very long cement glands and truncated cylindrical anterior proboscis with slight posterior dilation. There are over 98 valid species of *Centrorhynchus* Lühe, 1911 known from birds throughout the world (Amin, 2013). Much of the early descriptions of *Centrorhynchus globocaudatus* (Zeder, 1800) Lühe, 1911 (Centrorhynchidae) by Zeder (1800) and Rudolphi (1802) were repeated by subsequent observers. The distribution of *C. globocaudatus* appears to extend throughout Europe, Asia and Africa in many species of birds of prey of the genera *Anthus* Bechstein (Pipits), *Aquila* Brisson (true eagles), *Asio* (Linnaeus) (typical owls); *Athene* Boie (owls), *Buteo* Lacépède (buzzards), *Circus* Lacépède (harrier-hawks), *Falco* Linnaeus (falcons and kestrel), *Glaucidium* Boie (pigmy owls), *Milvus* Lacépède (kites), *Ottus* Pennant (Eurasian, Old World, scops owls), *Strix* Linnaeus (wood owls) and *Tyto* Billberg (barn owls) (see Petrochenko, 1950, 1958; Florescu & Ienistea, 1984; Hoklova, 1986; Lisitsyna, 2019). Insects serve as intermediate hosts for species of *Centrorhynchus*, while amphibians, reptiles and occasionally insectivorous mammals serve as second intermediate or paratenic hosts. Nelson & Ward (1966) collected juvenile specimens of *C. globocaudatus* from the long-eared hedgehog, *Hemiechinus auritus* Gmelin, in the Egyptian El Tahreer Province, and Torres & Puga (1966) collected cystacanths of specimens of *Centrorhynchus*

© The Author(s), 2020. Published by Cambridge University Press. This is an Open Access article, distributed under the terms of the Creative Commons Attribution licence (<http://creativecommons.org/licenses/by/4.0/>), which permits unrestricted re-use, distribution, and reproduction in any medium, provided the original work is properly cited.

Table 1. Collections of *Centrorhynchus globocaudatus* from *Falco tinnunculus* and *Buteo buteo* upon death at the Experimental Zooprophyllactic Institute of Ferrara, Italy, in 2018 and 2019.

Month	<i>Falco tinnunculus</i>		<i>Buteo buteo</i>		Location in Ferrara
	Juveniles	Adults	Juveniles	Adults	
June 2018	0/0	3/3 (11) ^a	0/0	0/0	Masi Torello, Cona
July 2018	1/1 (4)	1/2 (10)	0/0	0/0	Copparo, Contrapò, Ferrara
August 2018	0/2 (14)	1/1 (26)	0/0	0/0	Copparo, Ferrara, Fiscaglia
September 2018	0/0	0/0	0/0	0/0	—
October 2018	0/0	2/2 (4)	1/1 (11) ^b	1/1 (12)	Portomaggiore Formignana, Quartiere, Gualdo, Voghiera Vigarano
November 2018	0/0	0/0	0/0	0/0	—
December 2018	0/0	0/0	1/1 (2)	0/0	Rovigo
January 2019	0/0	0/0	0/0	1/1 (7)	Cordea
August 2019	0/0	2/2 (41)	0/0	0/0	Bondeno, Portomaggiore
Total	1/3 (18)	9/10 (92)	2/2 (13)	2/2 (19)	Ferrara Province

^aNumber of birds infected/number examined (acanthocephalans collected).

^bThese may be specimens of *C. globocaudatus*, but their identity could not be verified because of extreme contraction.

sp. from two species of frogs in Chile – *Eupsophus calcaratus* Günther and *Eupsophus roseus* Dumeril.

Reasonably adequate versions of the description of *C. globocaudatus* by these authors from Ukraine, Kyrgyzstan and former Soviet states, respectively, among others listed in table 1, were used for comparison with our Italian specimens. Other brief descriptions usually based on one or two male or female specimens were also reported from other localities in Bulgaria (Dimitrova et al., 1997), Hungary (Dimitrova et al., 1995), India (Gupta & Gupta, 1972), Slovakia (Komorová et al., 2015) and West Africa (Dimitrova & Gibson, 2005). The brief descriptions in Meyer (1932) and Yamaguti (1963) are worth noting. Two reports on synanthropic birds and their parasites in southern Italy by Dipineto et al. (2013) and Santoro et al. (2010) made reference to *C. globocaudatus* from the common kestrel, *Falco tinnunculus* Linnaeus, but no descriptive accounts are known for this acanthocephalan from Italy. Our descriptive account is based on collections from northern Italy at Ferrara. Our findings on *C. globocaudatus* recognize a new morphological variant and add new descriptive information that expands our understanding of this interesting acanthocephalan. For instance, the anterior five sub-apical hook roots were each found to be unique in shape and size rather than appearing identical, as has been noted in previous reports using only line drawings.

As usual in most acanthocephalan families, few sequences are available for centrorhynchids. For *C. globocaudatus*, only two sequences, corresponding to 18S and 28S ribosomal DNA (rDNA) genes, have been published to date (García-Varela et al., 2020a). If we consider published sequences of the genus, the number can be only expanded to six for the 18S gene, and even fewer sequences (4) are available for cytochrome *c* oxidase 1 (*cox1*).

In the present study, new scanning electron microscopy (SEM) and microscopic images, energy dispersive X-ray analysis (EDXA), micropore and related studies, and DNA analysis expand the body of knowledge about *C. globocaudatus* in particular and the genus *Centrorhynchus* in general.

Materials and methods

Collections

The birds examined for this study were collected between June 2018 and August 2019 from the countryside or villages around Ferrara (44°50'N, 11°37'E). Moribund birds injured in car accidents or those unable to fly are first brought to Centro Recupero Fauna Selvatica (Center for Recovery of Wild Fauna) (CRAS), often with police (Section of Wild Fauna) intervention, for first aid, and are hospitalized with a unique CRAS number. If the birds do not recover or die, they are sent to the Experimental Zooprophyllactic Institute of Ferrara at St Modena for necropsy, recovery of parasites and identification of possible infectious agencies such as West Nile Virus, then incinerated.

A total of 110 clearly identifiable specimens of *C. globocaudatus* were collected from 13 infected common kestrels (falcons), *F. tinnunculus*, and 32 from four infected common buzzard, *Buteo buteo* (table 1). Specimens from both host species were examined as follows: 16 specimens for SEM and EDXA, six for molecular analysis (three from each host species) and 12 males and 13 females (nine and ten from *F. tinnunculus*, and three and three from *B. buteo*, respectively) for microscopical study. Other specimens remain in O.M.A.'s personal collection. Freshly collected specimens were extended in water until proboscides everted then fixed in 70% ethanol for transport to our Arizona, USA laboratory for processing and further studies.

Methods for microscopical studies

Worms were punctured with a fine needle and subsequently stained in Mayer's acid carmine, destained in 4% hydrochloric acid in 70% ethanol, dehydrated in ascending concentrations of ethanol (24 h each) and cleared in 100% xylene then in 50% Canada balsam and 50% xylene (24 h each). Whole worms were then mounted in Canada balsam. Measurements are in micrometres, unless otherwise noted; the range is followed by the mean values between parentheses. Width measurements represent

maximum width. Trunk length does not include proboscis, neck or bursa.

Microscope images were created using 10× and 40× objective lenses of a BH2 light Olympus microscope (Olympus Optical Co., Osachi-shibamiya, Okaya, Nagano, Japan) attached to an AmScope 1000 video camera (United Scope LLC, dba AmScope, Irvine, California, USA), linked to an ASUS laptop equipped with a high-definition multimedia interface system (Fremont, California, USA). Images from the microscope are transferred from the laptop to a USB and stored for subsequent processing on a computer.

Specimens were deposited in the University of Nebraska State Museum's Harold W. Manter Laboratory (HWML) under collection number 139,404 (voucher specimens on one slide), Lincoln, Nebraska, USA.

SEM

Specimens that had been fixed and stored in 70% ethanol were processed for SEM following standard methods (Lee, 1992). These included critical-point drying in sample baskets and mounting on SEM sample mounts (stubs) using conductive double-sided carbon tape. Samples were coated with gold and palladium for 3 min using a Polaron #3500 sputter coater (Q150 TES, Quorum: www.quorumtech.com) establishing an approximate thickness of 20 nm. Samples were placed and observed in an FEI Helios Dual Beam Nanolab 600 (FEI, Hillsboro, Oregon, USA) scanning electron microscope, with digital images obtained in the Nanolab software system (FEI, Hillsboro, Oregon, USA) and then transferred to a USB for future reference. Samples were received under low vacuum conditions using 10 KV, spot size 2, 0.7 torr using a gaseous secondary electron detector.

EDXA

Standard methods were used for preparation similar to the SEM procedure. Specimens were examined and positioned with the aforementioned SEM instrument, which was equipped with a Phoenix energy-dispersive X-ray analyser (FEI, Hillsboro, Oregon, USA). X-ray spot analysis and live scan analysis were performed at 16 Kv with a spot size of 5, and results were recorded on charts and stored with digital imaging software attached to a computer. The TEAM (Texture and Elemental Analytical Microscopy) software system (FEI, Hillsboro, Oregon, USA) was used. Data were stored in a USB for future analysis. The data included weight percent and atom percent of the detected elements following correction factors.

Ion sectioning of hooks

A dual-beam SEM with a gallium (Ga) ion source (GIS) was used for the liquid metal ion source (LMIS) part of the process. The hooks of the acanthocephalans were centred on the SEM stage and cross-sectioned using a probe current of between 0.2 nA and 2.1 nA according to the rate at which the area was cut. The time of cutting was based on the nature and sensitivity of the tissue. Following the initial cut, the sample also underwent a milling process to obtain a smooth surface. The cut was then analysed with X-ray at the tip, middle and base of hooks for chemical ions with an electron beam (Tungsten) to obtain an X-ray spectrum. Results were stored with the attached imaging software.

The intensity of the GIS was variable according to the nature of the material being cut.

Molecular methods

Total genomic DNA (gDNA) was extracted from four specimens of *C. globocaudatus* (two ex. *B. buteo* and two ex. *F. tinnunculus*) preserved in ethanol 70% using a Qiagen™ (Valencia, California, USA) DNeasy® Tissue Kit and following the manufacturer's instructions. Partial nuclear small subunit (SSU) rDNA (18S rDNA) and partial fragments of mitochondrial *cox1* gene were amplified (50 µl total volume) using ExcelTaq™ SMOBIO® PCR Master Mix (Taiwan) containing 5× concentrated master mix – that is, a mixture of recombinant Taq DNA polymerase, reaction buffer, magnesium chloride (2 mM), deoxynucleotide triphosphates (dNTPs) (0.2 mM) and enzyme stabilizer; 0.25 µM of each polymerase chain reaction (PCR) primer and 2 µl of extracted gDNA. Primer pairs and amplification conditions used for both genes were as described in Amin *et al.* (2019a). In every PCR run, one negative and one positive control were included. PCR amplicons were sequenced directly for both strands using the same PCR primers.

Sequences were assembled and edited using ContigExpress implemented in the software Vector NTI Advance® version 10.3.0 (Thermo Fisher Scientific, Massachusetts, U.S.) and submitted to GenBank under accession numbers MT993836–MT993837 (18S rDNA) and MT992255–MT992256 (COI). Sequences were aligned using Muscle implemented in MEGA version 6 (Tamura *et al.*, 2013), together with all published 18S and *cox1* sequences of species within the family Centrorhynchidae available in GenBank. Detailed data on the sequences used on both alignments and phylogenetic reconstructions can be found in table 2. *Echinorhynchus truttae* Schrank, 1788 (Echinorhynchidae) was used as outgroup in both datasets (AY830156 and FR856883 in 18S and *cox1* datasets, respectively). Both alignments (18S: 764 nt positions, of which four were excluded prior to analysis; *cox1*: 668 nt positions, of which 29 were excluded prior to analysis) were used for comparative sequence analysis.

Gblocks 0.91b implemented on the Phylogeny.fr site (Dereeper *et al.*, 2008) was used to select blocks of evolutionarily conserved sites. Maximum likelihood (ML) and Bayesian inference (BI) algorithms were used for phylogenetic tree reconstruction after determination of the best-fit model of nucleotide substitution with jModelTest version 2.1.4 (Darriba *et al.*, 2012) using the Akaike Information Criterion and the Bayesian Information Criterion, respectively. For the 18S dataset, the best-fitting model selected for the ML algorithm was the GTR + G model (nst = 6, rates = gamma, ngammacat = 4), while for BI it was K80 + G (nst = 2, rates = gamma, ngammacat = 4). For the *cox1* dataset, the best-fitting model selected for ML algorithm was the GTR + G model (nst = 6, rates = gamma, ngammacat = 4), while for BI it was HKY + G (nst = 2, rates = gamma, ngammacat = 4). ML analyses were performed in PhyML version 3.0 (Guindon *et al.*, 2010) with a non-parametric bootstrap of 100 replicates. BI analyses were carried out with MrBayes version 3.2.6 (Ronquist *et al.*, 2012) on the CIPRES Science Gateway version 3.3 (Miller *et al.*, 2010). Log likelihoods were estimated over 10,000,000 generations using Markov chain Monte Carlo searches on two simultaneous runs of four chains, sampling trees every 1000 generations. The first 25% of the sampled trees were discarded as 'burn-in', and a consensus topology and nodal support estimated as posterior probability values (Huelsenbeck *et al.*,

Table 2. Data for Centrorhynchidae sequences used in molecular alignments and phylogenetic reconstructions. All sequences were retrieved from GenBank (except those from the present study).

Species	GenBank ID		Location	Host species (Order: Family)	Reference
	18S	cox1			
<i>Centrorhynchus aluconis</i> (Müller, 1780)	MN057695		Unknown	<i>Strix aluco</i> (Strigiformes: Strigidae)	García-Varela et al. (2020a)
		KT592357	Czech Republic	<i>Strix aluco</i> (Strigiformes: Strigidae)	Gazi et al. (2016)
<i>Centrorhynchus clitorideus</i> (Meyer, 1931)		MT113355	Swabi, Khyber Pakhtunkhwa Province (Pakistan)	<i>Athene noctua</i> (Strigiformes: Strigidae)	Muhammad et al. (2020)
		MN661372	Swabi, Khyber Pakhtunkhwa Province (Pakistan).	<i>Athene noctua</i> (Strigiformes: Strigidae)	Zhao et al. (2020)
<i>Centrorhynchus conspectus</i> Van Cleave & Pratt, 1940	U41399		Unknown	Unknown	Near & Nadler (1995) ^a
<i>Centrorhynchus globirostris</i> Amin, Heckmann, Wilson, Keele & Khan (2015)	KM588206		Oderolal, Sindh Province (Pakistan)	<i>Centropus sinensis</i> (Cuculiformes: Cuculidae)	Amin et al. (2015)
<i>Centrorhynchus globocaudatus</i> (Zeder, 1800) Lühe, 1911	MN057696		Unknown	Unknown (bird of prey)	García-Varela et al. (2020a)
	MT993837	MT992256	Ferrara, Province of Ferrara (Italy)	<i>Falco tinnunculus</i> (Falconiformes: Falconidae)	Present study
	MT993836	MT992255	Ferrara, Province of Ferrara (Italy)	<i>Buteo buteo</i> (Accipitriformes: Accipitridae)	Present study
<i>Centrorhynchus microcephalus</i> (Bravo-Hollis, 1947) Golvan, 1956	AF064813		Unknown	<i>Crotophaga sulcirostris</i> (Cuculiformes: Cuculidae)	García-Varela et al. (2000)
<i>Centrorhynchus milvus</i> Ward, 1956		MK922344	Swabi, Khyber Pakhtunkhwa Province (Pakistan)	<i>Milvus milvus</i> (Accipitriformes: Accipitridae)	Muhammad et al. (2019)
<i>Centrorhynchus nahuelhuapensis</i> Steinauer, Flores and Rauque (2019)	MK411249		Patagonia (Argentina)	<i>Strix rufipes</i> (Strigiformes: Strigidae)	Steinauer et al. (2019)
<i>Centrorhynchus nickoli</i>	MT161621		Veracruz (Mexico)	<i>Didelphis virginiana</i> (Didelphimorphia: Didelphidae)	García-Varela et al. (2020b)
<i>Centrorhynchus</i> sp.	AY830155	DQ089716	Unknown	<i>Falco peregrinus</i> (Falconiformes: Falconidae)	García-Varela & Nadler (2005)
<i>Sphaerirostris lanceoides</i> (Petrochenko, 1949)		MT476588	Swabi, Khyber Pakhtunkhwa Province (Pakistan)	<i>Ardeola grayii</i> (Ciconiiformes: Ardeidae)	Muhammad et al. (2020)
		MG931939	Yuyao, Zhejiang Province (China)	<i>Bufo gargarizans</i> (Bufonidae) ^b	Kang & Li (2018)
<i>Sphaerirostris picae</i> (Rudolphi, 1819)		MK471355	Swabi, Khyber Pakhtunkhwa Province (Pakistan)	<i>Dendrocitta vagabunda</i> (Passeriformes: Corvidae)	Muhammad et al. (2019)

^aDirect submission in GenBank.^bAcanthocephalans retrieved from their amphibian intermediate/paratenic host.

2001) were calculated from the remaining trees. Pairwise genetic distance matrices were calculated using the ‘uncorrected p-distance’ model implemented in MEGA version 6.

Results

The distribution of *C. globocaudatus* is known from at least ten genera of birds of prey in Europe, Asia and Africa (table 3). Our Ferrara, Italy, population of *C. globocaudatus* became available as a result of the regional monitoring of birds of prey to assess

the health of wild fauna and to identify the risk of parasitic and infectious agents, especially West Nile virus, for domestic animals, farm animals and humans. Our collection (table 1) shows a markedly higher intensity of infection in *F. tinnunculus* than in *B. buteo*, but rather similar prevalence rates. The comparable feeding modality of both bird species, mostly on young mammals like voles, less frequently on game and passerine birds, lizards, snakes, frogs, toads and invertebrates like arthropods, may be at play (Bergman, 1961; Cramp & Brooks, 1992; Viitala et al., 1995).

Table 3. Morphometric comparisons of key taxonomic characters between populations of *Centrorhynchus globocaudatus* from various bird hosts in different geographical locations in Asia, Europe and Africa.

Reference	Present paper	Lisitsyna (2019), Lisitsyna Greben (2015)	Petrochenko (1950, 1958)	Bhattacharya (2000, 2006), Naidu (2012)	Ward (1964) ^a	Hoklova (1986)
Locality	Ferrara (Italy)	Ukraine	Kyrgystan	Chandigarh, Punjab, Tripura, Sikkim (India)	Borg El Arab (Egypt)	Russia, Georgia, Armenia, other Asian Soviet republics
Host	<i>Falco tinnunculus</i> Linnaeus, <i>Buteo buteo</i> Linnaeus	<i>Falco tinnunculus</i> Linnaeus	<i>Falco tinnunculus</i> Linnaeus	<i>Milvus migrans</i> Boddaert, <i>Ottus</i> sp.	<i>Athene noctura</i> Scopoli	<i>Falco tinnunculus</i> Linnaeus, <i>Milvus migrans</i> Boddaert, <i>Buteo rufinus</i> (Cretzschmar), among others
Sample size	12 MM, 13 FF	7 MM, 14 FF,	—,—	—,—	11 MM, 12 FF	>11 MM, 12 FF, four juveniles
Males						
Trunk L × W (mm)	9.00–17.50 (13.05) × 0.50– 0.82 (0.65) ^b	11.95–18.8 (15.56) × 0.76–1.08 (0.93)	15.00–20.00 × 0.91– 1.00	15.00–20.00 × 0.90–1.31	15.00–18.00 × 0.8	15.00–20.00 × 0.80–1.00
Proboscis L × W	946–998 (977) × 364–426 (384) (posterior)	920–1,130 (1,050) × 300–354 (320) (anterior)	890–1,000 × 440 (posterior)	540–1,000 × 440 (posterior)	700–1,000 × 400 (posterior)	0.70–1.10 × 0.40–0.52 (posterior)
Hook rows × H/row	30 (30) × 19–21 (20)	30–34 (31) × 19–21 (20)	32–34 × 18	30–34 × 18–20	28–32 × 19–22	26–34 × 18–22
Longest hook L	50–55 (51), 57–65 (60) ^c	50–68 (57.6)	44^d	50	30–40 , 50–60	30–40 , 50–60
Proboscis receptacle L × W	1.40–1.92 (1.64) × 0.16–0.26 (0.21)	1.10–1.55 (1.26) × 0.23–0.37 (0.29)	1.27 × 0.31	1.27–1.40 × —	1.10–1.30 × 0.30–0.45	0.95–1.40 × 0.30–0.45
Lemnisci L × W (mm)	1.20–1.46 (1.31) × 0.08– 0.15 (0.12)	0.92–1.90 (1.50) × to anterior testis	1.36 × —	—	1.80–2.20 × 0.12	1.36–2.20 × 0.12
Anterior testis L × W	541–950 (806) × 200–450 (324)	730–1060 (910) × 430– 660 (500)	—	468 × 360	800–900 × 200– 300	800–900 × 200–300
Posterior testis L × W (mm)	575–975 (829) × 250–375 (311)	850–1080 (980) × 458– 660 (546)	—	—	800–900 × 200– 300	800–900 × 200–300
Cement gland L × W (mm)	3.50–6.45 (5.18) × 0.17– 0.27 (0.23)	7.83–11.08 (8.82) × —	8.25 × —	8.25 × 0.22–0.36	9.00–12.00 × 0.10	8.25–12.00 × 0.10
Cement gland duct L (mm)	2.00–3.00 (2.50) × 0.12– 0.30 (0.18)	—	2.45 × —	2.45 × —	2.45 × —	—
Saeffligen's pouch. L × W (mm)	1.62–2.50 (2.29) × 0.20– 0.37 (0.26)	1.40–2.65 (2.21) × —	—	2.52 × 0.29	—	—
Bursa L × W (mm)	1.00 × 0.87 (n = 1)	2.00 × 1.30	—	0.74 × 1.10	—	—
Females						
Trunk L × W (mm)	23.12–38.75 (29.94) × 0.70–0.90 (0.80) (anterior) 0.72–1.39 (0.96) (posterior)	15.01–40.00 (20.18) × 0.80–1.40 (1.06)	37.00–55.00 × — 1.10–1.50 (posterior)	21.00–55.00 × — —	20.00–35.00 × 1.00 —	20.00 × 55.00 × 1.00–1.50 1.10–1.50

(Continued)

Table 3. (Continued.)

Reference	Present paper	Lisitsyna Greben (2015), Lisitsyna Greben (2019),	Petrochenko (1950, 1958)	Bhattacharya (2000, 2006), Naidu (2012)	Ward (1964) ^a	Hoklova (1986)
Proboscis L × W	1.00–1.29 (1.10) × 0.41–0.47 (0.44) (posterior)	0.92–1.18 (1.06) × 0.30–0.40 (0.34) (anterior)	1.00–1.10 × 0.40–0.52 (posterior)	—	0.70–1.00 × 0.40 (posterior)	0.70–1.10 × 0.40–0.52 (posterior)
Hook rows × H/row	29–33 (31) × 19–22 (21)	30–36 (33) × 19–21 (19.8)	34 × 18–19	30–32 × 18–20	28–32 × 19–22	26–34 × 18–22
Longest hook L	50–57 (54), 57–70 (64)	50–65 (60.7)	44	—	30–40 , 50–60	30–40 , 50–60
Proboscis receptacle L × W (mm)	1.72–2.44 (2.05) × 0.22–0.36 (0.28)	1.16–1.62 (1.3) × 0.25–0.41 (0.36)	1.40 × 0.38	—	1.10–1.30 × 0.30–0.45	0.95–1.40 × 0.30–0.45
Lemnisci L × W (mm)	1.50 × 0.11 (n = 1)	0.92–2.05 (1.66) × —	—	—	1.80–2.20 × 0.12	1.36–2.20 × 0.12
Eggs L × W	45–52 (49) × 20–25 (22)	53–60 (56) × 24–30 (28)	49–55 × 22	42–55 × 21–22	40–60 × 20	40–60 × 20–22

L: length, W: width, H: hook.

^aExcept for size of trunk, Ward (1964) provided only one set of measurements and counts for both male and female specimens.

^bRange (mean) in micrometres unless otherwise noted.

^cLargest dorsal hook length, largest ventral hook length. Longest hook length is used as an indicator of the size of all hooks for comparative purposes with specimens from other collections.

^dBolded figures markedly vary from those of our Italian specimens.

We describe our northern Italian population morphologically as a geographical variant because of its distinct variability from other descriptive accounts elsewhere where information is available. Descriptive reports variably document its morphology using only line drawings. Among these, we consider the line drawings in Petrochenko (1950) and Lisitsyna & Greben (2015) to be the most complete and adequately representative. Minor exceptions are noted. We, therefore, opted not to duplicate these line drawings of the species and, instead, produce SEM and microscope images for the first time for documentation and introduce new information on the EDXA to discern hook metal composition, Ga hook cuts, micropores and molecular analysis for the first time. Additional details of such structures as proboscis hook roots are described and inaccuracies and errors are being corrected.

The following morphological description is based on the microscopical examination of 25 specimens (12 males, 13 females) and others used in the SEM studies. These study specimens were collected from the common kestrel, *F. tinnunculus* (19 specimens), and the common buzzard, *B. buteo* (six specimens), and a complete set of measurements of each were made before later collections in 2019 were made.

Morphological description of our population from Ferrara Province, Italy

Centrorhynchus globocaudatus (Zeder, 1800) Lühe, 1911 (figs 1–3, 4a–d)

General. With characters of the genus *Centrorhynchus* and the family Centrorhynchidae, as defined by Amin et al. (2015). Shared structures markedly larger in females than in males (table 3). Trunk long, cylindrical, slightly wider anteriorly in males and with prominent posterior swelling and terminal knob in females. Cuticle with cross-striations, especially anteriorly, and lacunar system with prominent transverse secondary lacunar canal. Body wall with many fractured nuclei, and micropores with diverse diameter and distribution in different trunk regions (fig. 2d–f). Proboscis elongate cylindrical, gradually widening posteriorly (fig. 1a), apically truncated and bare (fig. 1b), but apical organ occasionally evident by its anterior invagination (fig. 1c, d). Proboscis widening posteriorly past faint constriction at point of attachment of receptacle. Proboscis with 29–33 longitudinal rows of 19–22 hooks each. Anterior 5–7 hooks strongest (fig. 1e), with prominent core and thin cortical layer (fig. 2b, c) and prominent posteriorly directed roots variable in shape and size (fig. 5b); third or fourth hooks longest. Ventral surface of hooks with many pebble-like protrusions, especially near base (fig. 1f). Next 5–7 hooks transitional, spiniform, with prominent scutiform X-shaped roots at area of receptacle attachment near proboscis constriction. Subsequent posterior spiniform hooks (fig. 2a) with smaller scutiform roots becoming simpler and directed anteriorly in posteriormost hooks. Anterior hooks appear in alternating longitudinal rows, but they and all spiniform hooks also appear in definite spiral rows (fig. 1a). Neck relatively short with clear cuticular separation from basal proboscis region (fig. 2a). Proboscis receptacle (PR) double-walled, about twice as long as proboscis in females (c. 1.5 as long in males) with cephalic ganglion near its middle at level of anteriormost margin of trunk. PR inserts anteriorly near anterior third of proboscis where anterior robust hooks transform into

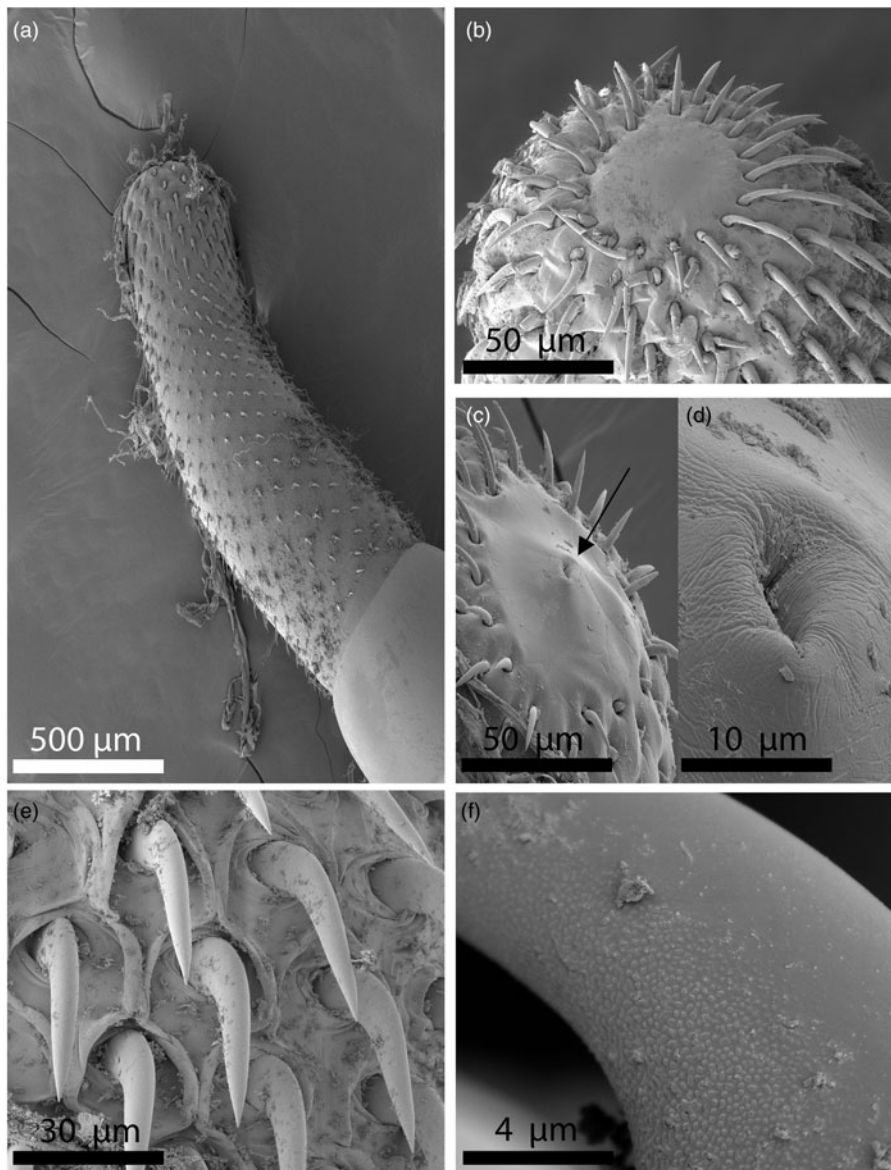


Fig. 1. SEM of specimens of *Centrorhynchus globocaudatus* from *Falco tinnunculus* and *Buteo buteo* from northern Italy at Ferrara. (a) The proboscis of a female specimen. Note the spiral pattern of the longitudinal hook rows. (b) The anterior end of a proboscis showing the bare apical surface. (c) The sensory pore is more visible (arrow) at the apical end of another proboscis in occasional specimens. (d) A higher magnification of the sensory pore in (c). (e) A series of anterior hooks. Smaller apical hooks are more anterior. (f) A high magnification of a hook near its base showing latero-ventral pebble-like protrusions.

transitional spiniform hooks at faint constriction. Lemnisci saciform, equal, slightly shorter than receptacle but may reach level of anterior testis.

Males (based on 12 mature specimens with sperm). See table 3 for measurements and counts. Testes in anterior fifth of trunk, in tandem, not large, elliptical, nearly equal, contiguous or slightly overlapping. Four cement glands, tubular, tightly contiguous, often appearing as long cord, staggering anteriorly at posterior testis and extending posteriorly into prominent cement gland ducts (CGDs) (fig. 5b) discharging into bursa. Robust Saeftigen's pouch prominent, elongate-drop-shaped, widest anteriorly, contiguous with posterior end of cement glands (fig. 5c) and overlapping CGDs. Bursa large, longer than wide, with oblong sensory pits in round elevated rims. Common sperm duct, cement glands duct and Saeftigen's pouch jointly end in bursa. Gonopore terminal.

Females (based on 13 gravid adults). Few females had ovarian balls. See table 3 for measurements and counts. Posterior end of trunk inflating abruptly then constricting into terminal prominent papilla (fig. 3a, b). Female reproductive system largely masked

by dark eggs, usually in two lateral fields along worm length. Vagina complex, subterminal, with three sphincters and slit orifice opening at base of terminal globular papilla. Wall of papilla thick, continuous with body wall, with prominent muscle band holding dorsal and ventral sides together (fig. 5d, arrow). Uterus comparatively long; uterine bell short with few but prominent cells. Eggs ovoid, with thick concentric shells, and surface varying between smooth (fig. 3c) and tuberculated (fig. 3d), with occasional sperms evident (fig. 3e). Three eggshells evident (arrows) and embryonic acanthor and its components seen in Ga-cut sections (fig. 3f).

Taxonomic summary

Italian hosts examined. The common kestrel, *F. tinnunculus* Linnaeus (Falconidae), and the common buzzard, *B. buteo* Linnaeus (Accipitridae).

Locality. Around Ferrara (44°50'N, 11°37'E), Province of Ferrara, Italy.

Localization. Intestine.

Specimens deposited. HWML collection number 216359.

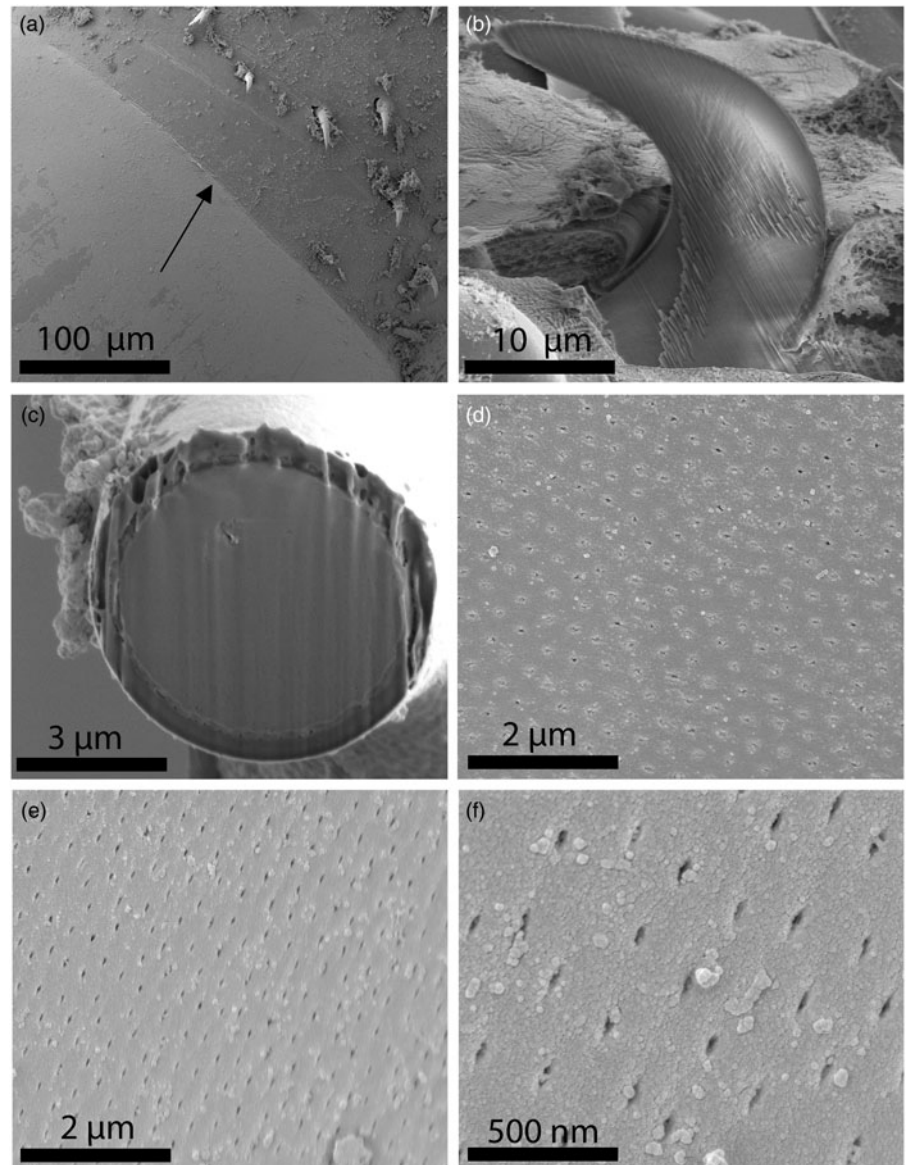


Fig. 2. SEM of specimens of *Centrorhynchus globocaudatus* from *Falco tinnunculus* and *Buteo buteo* from northern Italy at Ferrara. (a) The distinct interface between the posterior end of a proboscis near a basal circle of small hooks and the neck. The arrow points to the interface between the proboscis and the neck. (b) A lateral view of a Ga-cut hook showing the solid prominent core and very thin cortical layer. (c) A cross section of another hook demonstrating the layering showed in (b). (d, e) Micropores of different sizes, distribution and shape in the anterior and middle trunk of a male specimen, respectively. (f) A higher magnification of micropores in (e) display their unusual elliptical elongated shape.

EDXA

The unique metal composition of hooks (EDXA) (tables 4–6 and figs 6–10) demonstrated a considerably high level of calcium and phosphorus in hook tip, a middle but low level of sulphur and negligible levels of other metals (table 4 and figs 6, 7). The eggs had the highest levels of sulphur in the cortical and core areas, but high levels of phosphorus only in the core and not in the cortical layer (table 6 and fig. 10).

Micropores

The electron-dense micropores present throughout the epidermal surface of the trunk of *C. globocaudatus* are described. They have been found in various regions of the trunk in different diameters and distributions (fig. 4a, b).

Molecular results

Two identical partial 18S rDNA sequences (760 and 833 nt length) and two *cox1* mitochondrial DNA (mtDNA) sequences (651 and 668 nt length) differing by 1 nt (0.16% divergence) were generated, one from each host (i.e. *B. buteo* and

F. tinnunculus). Figures 11 and 12 display consensus trees constructed from 18S rDNA and *cox1* alignments, respectively.

According to phylogenetic analyses based on the 18S rDNA gene (fig. 11), present newly generated sequences were identical to that of *C. globocaudatus* published by García-Varela *et al.* (2020a) (MN057696). Therefore, these three sequences formed a strongly supported clade. The sequences that differed the most from this clade corresponded to *Centrorhynchus nickoli* (MT161621) and *Centrorhynchus microcephalus* (AF064813) (by 0.051 and 0.045% (39 and 34 nt), respectively), although the rest of the *Centrorhynchus* 18S sequences differed from newly generated sequences by 0.033–0.041% (25–31 nt) (table 7).

In phylograms based on the *cox1* gene, present sequences formed a well-supported clade apart from all other centrorhynchid sequences included in the analyses (fig. 12). The only other clade displaying high support included *Sphaerirostris* sequences, with 11–30 nt (0.017–0.047%) difference among them, and was embedded among *Centrorhynchus* sequences forming a sub-clade. However, nucleotide difference highly increased if *Sphaerirostris* sequences are compared with newly generated ones (0.248–

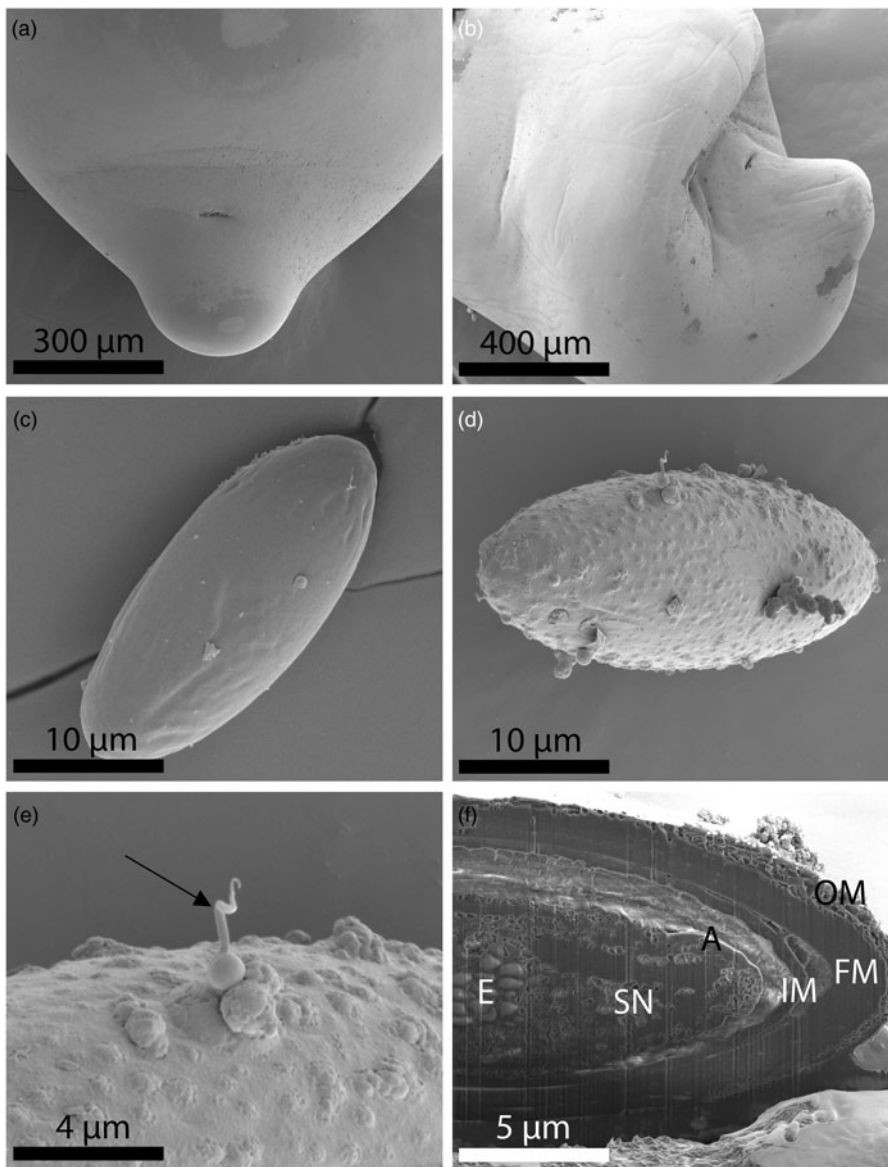


Fig. 3. SEM of female reproductive structures of specimens of *Centrorhynchus globocaudatus* from *Falco tinnunculus* and *Buteo buteo* from northern Italy at Ferrara. (a) The broad posterior portion of a female specimen showing the sub-ventral position of the gonopore where the trunk narrows into a terminal caudal papilla. (b) A lateral view of the enlarged posterior portion of a female trunk and the common dorsal curvature commonly described as shoe-like. (c) Egg with smooth surface. (d) Egg with tuberculated surface, which may be at a different stage of development. (e) A high magnification of a portion of the egg in (d) showing a sperm (arrow). (f) Part of a Ga-cut lateral section of an egg showing the following structures: A, acanthor; E, entoblast cells; FM, fertilization membrane; IM, inner membrane; OM, outer membrane; SN, subcuticular nuclei.

0.255%, 158–163 nt difference) and other species of the genus *Centrorhynchus* (0.194–0.264%, 124–169 nt; table 7). Other *Centrorhynchus* *cox1* sequences differed with present newly generated sequences by 0.250–0.277% (160–177 nt; table 7), and showed very weakly supported phylogenetic relationships.

Remarks

A morphometric comparison between our Italian specimens and those from other geographical locations where comparative measurements and counts were available is shown in table 3. *Centrorhynchus globocaudatus* has been reported from many other locations in Asia, Africa and Europe without taxonomic descriptions, leaving their morphologic variability unaccounted for. Most measured specimens were collected from *F. tinnunculus*, thus eliminating host species as a factor in observed differences in sizes (table 3). Our specimens had markedly longer proboscis hooks and larger receptacle, and smaller male reproductive system (testes and cement glands) and lemnisci, especially in males compared to specimens from Ukraine, India, Egypt, Kyrgyzstan,

Russia, Georgia, Armenia and Asian Soviet Republics. The Indian specimens probably had an erroneous testis size of 468×360 . Additionally, females from Ukraine and Kyrgyzstan had more proboscis hook rows, and those from Ukraine had relatively larger eggs (table 3). Such quantitative variations distinguishing the Italian population as a geographical variant have been previously demonstrated in the comparable case of *Mediorhynchus papillosus* Van Cleave, 1916 (Gigantorhynchidae) by Amin & Dailey (1998). Amin & Dailey (1998) studied the key taxonomic characteristics in various geographical populations of *M. papillosus*, which has a wide range of distribution in at least 73 species of birds outside of North and South America in Asia from Taiwan to the east into China, many of the former Soviet Republics and to Eastern Europe to the west. Amin & Dailey (1998) compared measurements of specimens from birds in Maryland, Colorado (their study material), Taiwan, Yakutia, Trans-Baikal, Lower Yansi River basin, the Volga basin and Oren Byreg, Ukraine, Bulgaria, China and Brazil, and demonstrated a distinct geographically based variability, especially in the size of proboscis and its armature, neck,

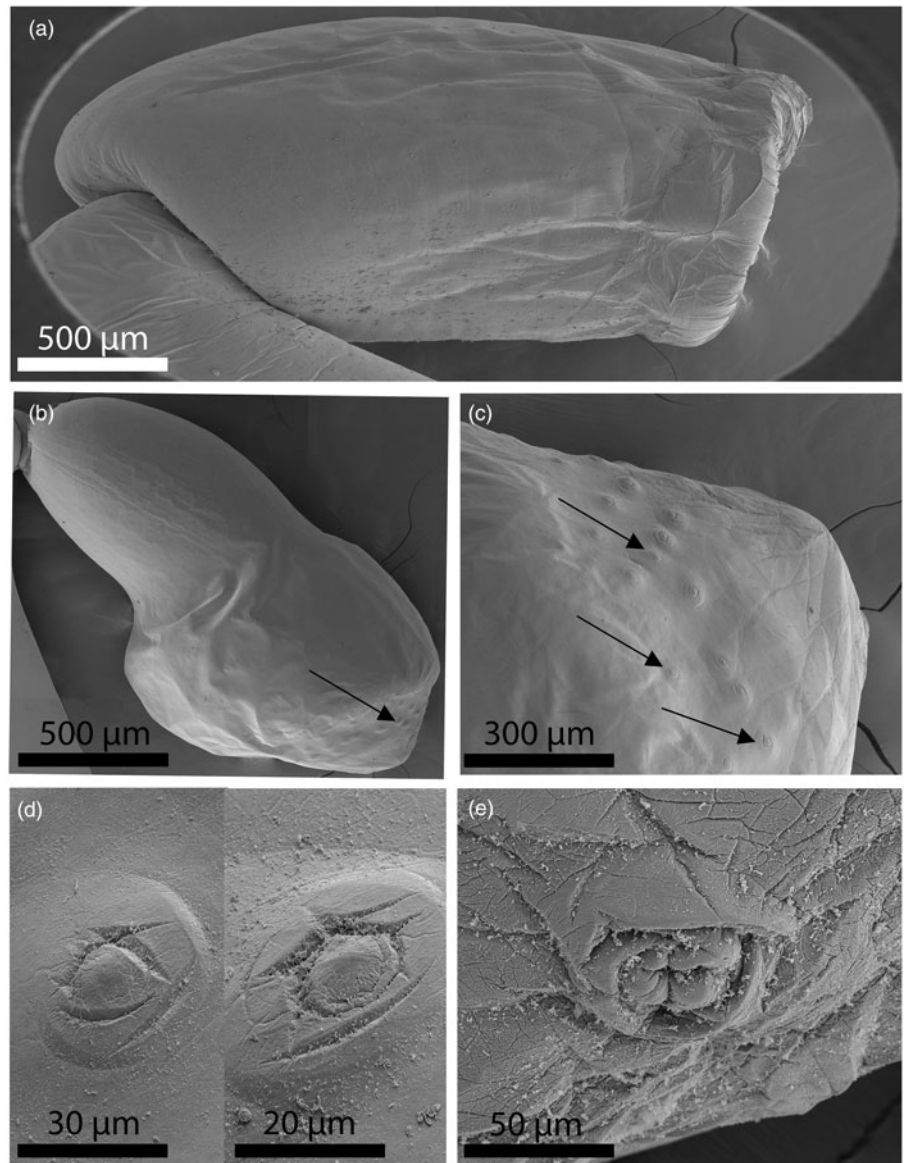


Fig. 4. SEM of the male reproductive structures of specimens of *Centrorhynchus globocaudatus* from *Falco tinnunculus* and *Buteo buteo* from northern Italy at Ferrara. (a) A lateral view of an extended elongated bursa. (b) A bursa bloated posteriorly showing the distribution of sensory plates only at its posterior end (arrow). (c) A high magnification of the bursa in (b) showing the distribution of the elevated ovoid sensory plates (arrows). (d, e) High magnifications of sensory plates showing their variable shapes, organization and elevation.

receptacle and testes, that appeared related to geographical restrictions, intermediate and definitive host specificity and distribution, and host feeding behaviour. ‘The U.S. population from Colorado and the Taiwanese population [were shown to be] at the opposite ends of the spectrum’ by Amin & Dailey (1998), who dismissed the possibility of elevating them to a specific status. The population variant of *C. globocaudatus* from Italy is, nevertheless, comparable to the east–west–intraspecific clinal variants of *M. papillosus* and could have been considered as a distinct species, but this notion is dismissed here also for the same reasons.

Discussion

A qualitative comparison between the Italian specimens and those from other geographical locations in table 1 and elsewhere shows discrepancies that may be related to artifacts or inaccuracy of recording observations. These discrepancies are to be expected considering the large number of descriptive accounts of this common acanthocephalan that have been reported since 1800. These discrepancies are rectified below to avoid misinterpretations of the

correct descriptive account of *C. globocaudatus*. Intraspecific variabilities, such as differences in the number of anterior, transitional and posterior spiniform hooks/row, will not be included.

Setting the record straight

- Lisitsyna & Greben (2015) stated that the proboscis has a ‘maximum width at the anterior part’ of males and females and their Fig. 3a shows a posterior proboscis constriction. The proboscis is actually widest posteriorly and Florescu & Ienistea (1984, Fig. 21) and our observations (fig. 1a) demonstrate this character best.
- Lisitsyna & Greben (2015) stated that ‘Gonopore subterminal in both sexes.’ Actually, the male gonopore is terminal (Fig. 20). The bend at the posterior end of the male trunk makes the gonopore appear subterminal.
- Nelson & Ward (1966) examined four juvenile specimens from the long-eared hedgehog, *H. auritus* Gmelin, from Egypt, showing a ‘nearly cylindrical’ proboscis also widest anteriorly (their

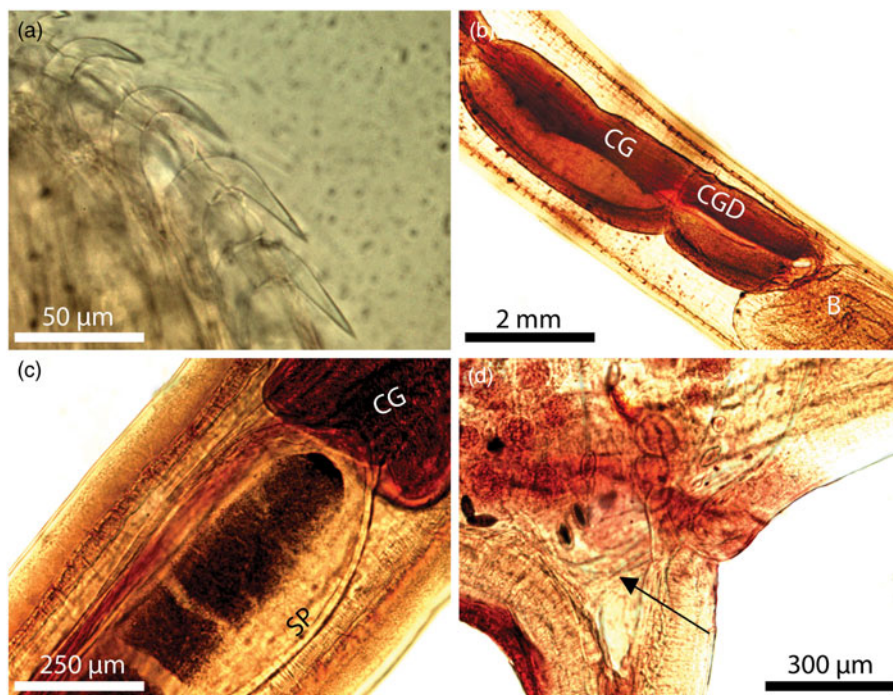


Fig. 5. Microscopic images of specimens of *Centrorhynchus globocaudatus* from *Falco tinnunculus* and *Buteo buteo* from northern Italy at Ferrara. (a) A lateral view of proboscis hooks showing their variable sizes and the variable shape and size of their roots. The roots vary in size and thickness antero-posteriorly. (b) The shape and size proportion of cement glands (CG) and CGD draining into the bursa (B). (c) The anterior end of Saeftigen's pouch (SP) overlapping the posterior end of the cement gland. (d) The posterior end of a female specimen showing the subterminal position of the gonopore, constriction of the body wall into the terminal papilla and the muscle band holding its dorsal and ventral sides together (arrow).

Table 4. Chemical composition of a Ga (LMIS)-cut hook (cross and longitudinal cuts) for *Centrorhynchus globocaudatus* using X-ray scans (EDXA).

Elements ^a	Cross-tip cut		Cross-mid cut		Long cut	
	Edge	Middle	Edge	Middle	Arch	Base
Sodium (Na)	0.06^b	0.11	0.05	0.08	0.15	0.07
Magnesium (Mg)	0.43	1.62	0.14	1.20	1.49	0.89
Phosphorus (P)	12.38	20.96	9.01	20.43	17.68	16.88
Sulphur (S)	4.38	0.30	1.81	0.17	0.06	0.23
Potassium (K)	0.09	0.16	0.15	0.17	0.17	0.75
Calcium (Ca)	29.99	46.59	25.26	48.26	40.19	50.01

^aCommon protoplasmic elements (C, N, O) and processing elements (Au, Pd, Ga) omitted. Given in WT%.

^bBolded figures are used to generate spectra in [figs 6 and 7](#).

Table 5. Chemical composition of tip cuts of hooks at three levels of proboscis of *Centrorhynchus globocaudatus* from *Falco tinnunculus*.

Elements ^a	Apical hook		Middle hook		Basal hook	
	Edge	Centre	Edge	Centre	Edge	Centre
Sodium (Na)	0.02	0.00	0.16	0.07^b	0.16	0.15
Magnesium (Mg)	0.70	1.02	0.37	1.06	0.37	0.23
Phosphorus (P)	11.37	18.96	8.65	16.44	8.65	3.60
Sulphur (S)	5.13	0.47	10.01	2.97	10.01	16.74
Potassium (K)	0.06	0.17	0.11	0.19	0.11	0.18
Calcium (Ca)	20.03	41.69	16.23	34.83	16.23	6.29

^aCommon protoplasmic elements (C, N, O) and processing elements (Au, Pd, Ga) omitted. Given in WT%.

^bBolded figures are used to generate spectra in [figs 8 and 9](#).

Table 6. Chemical composition of a Ga (LMIS)-cut egg of *Centrorhynchus globocaudatus* using X-ray scans (EDXA).

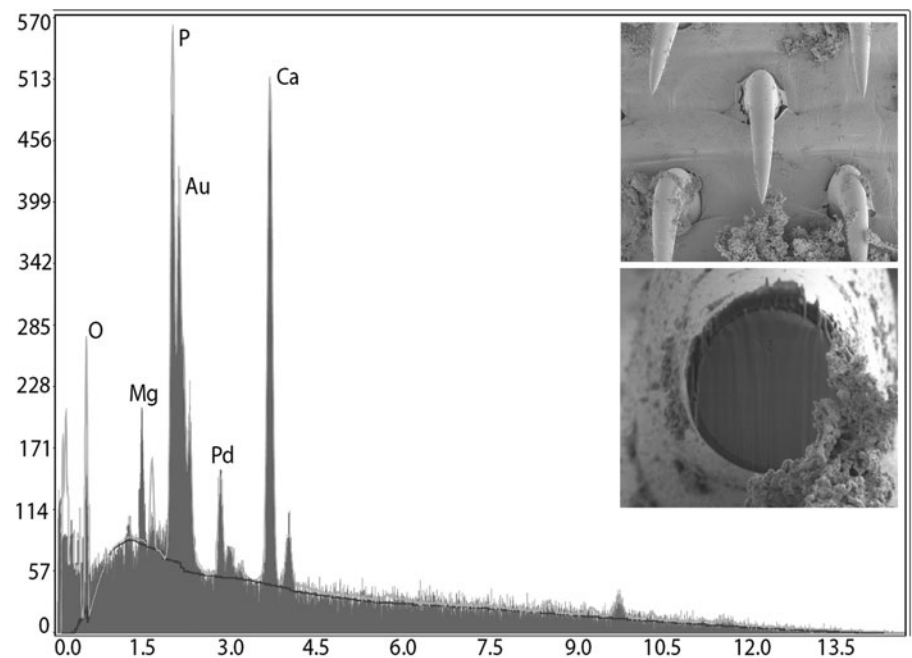
Elements ^a	Egg Edge	Egg middle
Sodium (Na)	0.45^b	0.01
Magnesium (Mg)	0.11	0.11
Phosphorus (P)	1.24	9.01
Sulphur (S)	12.94	8.04
Potassium (K)	0.11	0.34
Calcium (Ca)	0.47	0.71

^aCommon protoplasmic elements (C, N, O) and processing elements (Au, Pd, Ga) omitted. Given in WT%.

^bBolded figures are used to generate spectra in [fig. 10](#).

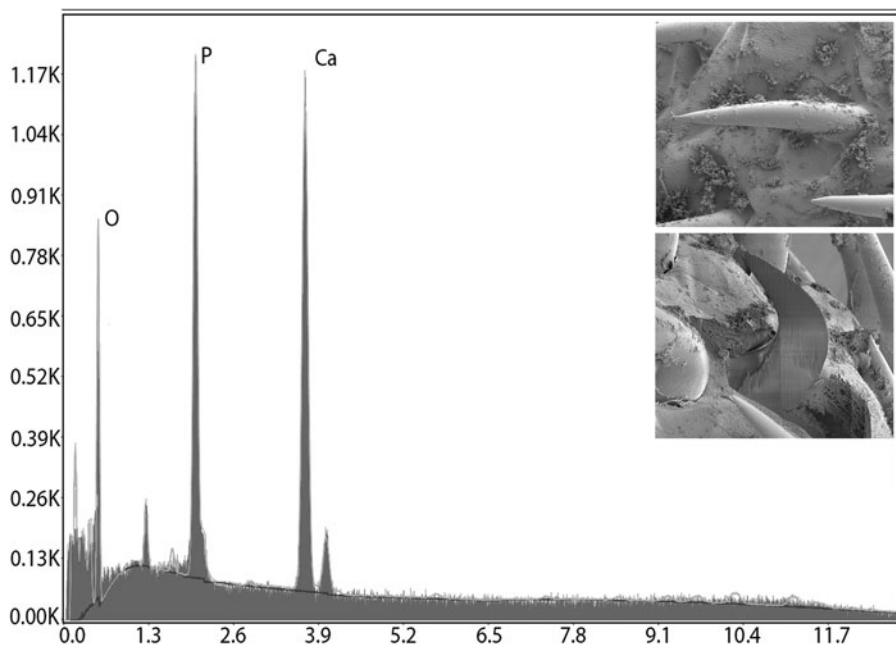
[Fig. 6](#)), with unusually few (26–28) longitudinal rows of 20–22 hooks each.

- Only Ward (1964) and the present paper document longer ventral and shorter dorsal proboscis hooks ([table 3](#)). All other accounts include only one set of measurements of hooks overlooking their dorso–ventro differentiation.
- Dimitrova *et al.* (1997), however, noted slightly longer latero-ventral hooks (60–65 long) than dorso-lateral hooks in one male worm from *F. tinnunculus*, but their other male worm from *Falco vespertinus* Linnaeus did not show such differentiation.
- Ward (1964) referred to spiniform hooks on the posterior proboscis as being ‘without roots.’ Actually, these hooks have small scutiform roots, becoming more simple and directed anteriorly in posteriormost hooks, as recognized in our Italian specimens and many other reports.



Element	Weight %	Atomic %	Error %	Net Int.	K Ratio
C	3.06	8.12	99.99	19.03	0.0140
N	9.96	22.68	15.64	30.02	0.0243
O	10.95	21.83	11.73	80.09	0.0319
Na	0.06	0.09	99.51	1.08	0.0004
Ga	0.06	0.03	57.15	0.54	0.0004
Mg	0.43	0.57	61.58	10.95	0.0030
P	12.38	12.75	5.77	279.62	0.1051
Au	21.53	3.49	9.24	197.67	0.1639
S	4.38	4.36	10.00	88.83	0.0352
Cl	0.05	0.04	99.99	0.80	0.0004
Pd	7.07	2.12	16.49	60.46	0.0489
K	0.09	0.07	99.99	1.23	0.0007
Ca	29.99	23.87	4.59	357.46	0.2523

Fig. 6. Energy dispersive X-ray spectrum of the edge of a cross GA-cut hook tip of a *Centrorhynchus globocaudatus* specimen showing high levels of calcium and phosphorus (see bolded figures in [table 4](#)). Insert: SEM of a middle proboscis hook and a GA-cut cross section of a hook.



Element	Weight %	Atomic %	Error %	Net Int.	K Ratio
C	2.73	5.42	99.99	27.88	0.0120
N	12.38	21.08	13.35	56.50	0.0267
O	22.61	33.70	9.70	260.09	0.0605
Na	0.15	0.16	70.01	4.26	0.0008
Ga	0.66	0.22	52.21	10.54	0.0046
Mg	1.49	1.46	10.88	62.27	0.0101
P	17.68	13.61	3.13	656.35	0.1439
Au	1.51	0.18	29.16	23.59	0.0114
S	0.06	0.04	99.99	2.00	0.0005
Cl	0.04	0.03	99.99	1.15	0.0003
Pd	0.34	0.08	59.85	5.14	0.0024
K	0.17	0.10	68.14	4.40	0.0015
Ca	40.19	23.91	2.93	815.08	0.3357

Fig. 7. Energy dispersive X-ray spectrum of a longitudinal GA-cut hook arch of a *Centrorhynchus globocaudatus* specimen showing high levels of calcium and phosphorus (see bolded figures in table 4). Insert: SEM of proboscis hooks and a longitudinal GA-cut section of a hook.

- Ward (1964) also stated that 'hard-shelled embryos of mature females elliptical, with middle membrane slightly evaginated at poles.' Such 'evagination' was not evident in our Italian specimens, nor has it been reported elsewhere.
- Gupta & Gupta (1972) studied one male worm from *Milvus migrans* in Chandigarh, India, and also reported four cement glands, which has been confirmed by Dezfuli *et al.* (2020) on histological grounds. It is easy to confuse the number of cement glands as they often appear to coalesce in one thick cord.
- Bhattacharya (2000) examined one male worm from *Ottus* sp. in Tripura, India, and reported '2 or 3' cement glands. Bhattacharya (2007) later reported four cement glands (see above).
- Bhattacharya (2000) also reported that second, third and fifth hooks from anterior are 'strongest.' This may be true for the fifth hook, but not likely the second or third.
- Gupta & Gupta (1972) created a very confused presentation of their work marred by erroneous interpretation of ordinary anatomical structures. They noted that the trunk is aspinose, but

indicate that the neck is 'short, rectangular and measures 0.180 × 0.378 mm. It is armed with 30 longitudinal rows of spines and 5–6 spines in each row.' Their Fig. 14 shows the PR inserting at the anterior end of their 'neck.' The authors clearly confused the posterior proboscis with a neck; not a common mistake.

- Gupta & Gupta (1972) further indicated that the posterior testis could not be measured because it was 'distorted.' However, their Fig. 13 clearly delineated a posterior testis as distinctly outlined as the anterior testis.
- Dimitrova *et al.* (1995) examined one male from *Falco cherrug* Gray in Hungary and reported 8–9 anterior hooks, with anteriormost hooks unusually long, 2–3 transitional hooks and 12–13 posterior spiniform hooks. Their disproportional and inaccurate Fig. 2, however, shows 9–10 hooks/row on an atypically spheroid anterior proboscis and only 2–5 spiniform hooks/row on the posterior proboscis.
- Dimitrova & Gibson (2005) examined only two female specimens. They indicated that 'posterior trunk terminates in

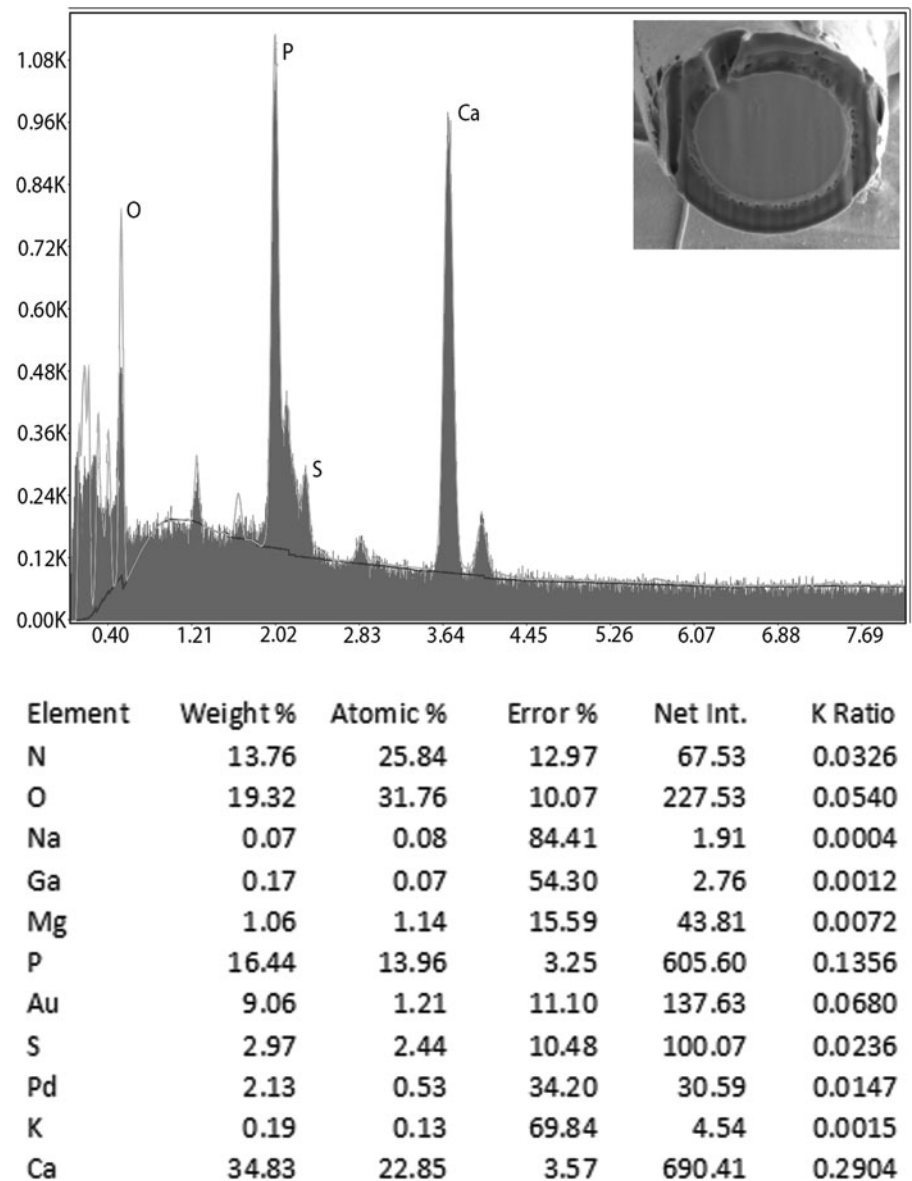


Fig. 8. Energy dispersive X-ray spectrum of the centre of a GA-cut middle hook of a *Centrorhynchus globocaudatus* specimen showing high levels of calcium and phosphorus (see bolded figures in table 5). Insert: SEM of a cross section of a middle proboscis hook.

rounded conical papilla,' but their Figs 6b and 2c of two female posterior ends show no such papillae. They also report 'vagina with 2 sphincters.' We find three vaginal sphincters.

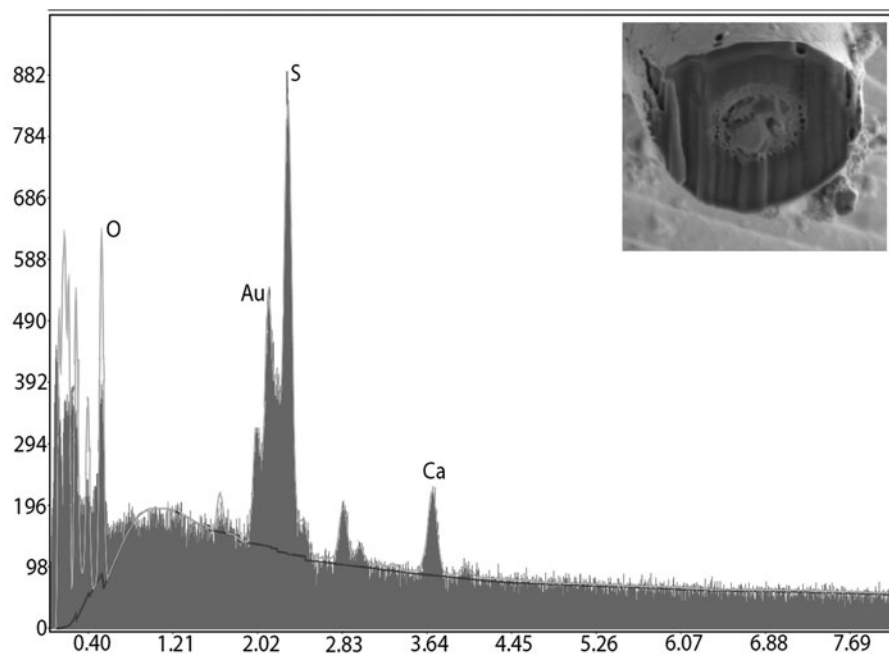
Micropores

The micropores of *C. globocaudatus*, like those reported from other species of the Acanthocephala, are associated with internal crypts and vary in diameter and distribution in different trunk regions corresponding to differential absorption of nutrients. We have reported micropores in a large number of acanthocephalan species (Heckmann et al., 2013) and in a few more since, and demonstrated the tunnelling from the cuticular surface into the internal crypts by transmission electron microscopy. Amin et al. (2009) gave a summary of the structural–functional relationship of the micropores in various acanthocephalan species including *Rhadinorhynchus ornatus* Van Cleave, 1918, *Polymorphus minutus* (Goeze, 1782) Lühe, 1911, *Moniliformis moniliformis* (Bremser, 1811) Travassos (1915), *Macracanthorhynchus hirudinaceus* (Pallas, 1781) Travassos (1916, 1917) and *Sclerocollum*

rubrimaris Schmidt & Paperna, 1978. Wright & Lumsden (1969) and Byram & Fisher (1973) reported that the peripheral canals of the micropores are continuous with canalicular crypts. These crypts appear to 'constitute a huge increase in external surface area . . . implicated in nutrient up take.' Whitfield (1979) estimated a 44-fold increase at a surface density of 15 invaginations per $1 \mu\text{m}^2$ of *M. moniliformis* (Bremser, 1811) Travassos, 1915 tegumental surface. The micropores and the peripheral canal connections to the canaliculi of the inner layer of the tegument of *Corynosoma strumosum* (Rudolphi, 1802) Lühe, 1904 from the Caspian seal *Pusa caspica* (Gmelin) in the Caspian Sea were demonstrated by transmission electron micrographs in Amin et al. (2011).

EDXA

Results of the X-ray scans of the Ga-cut hooks (dual-beam SEM) of *C. globocaudatus* show differential composition and distribution of metals in different hook parts, with calcium and phosphorus levels being highest at the middle of hook tip and mid



Element	Weight %	Atomic %	Error %	Net Int.	K Ratio
C	16.42	30.03	99.99	123.14	1.0638
N	17.68	27.73	12.55	89.69	0.0512
O	15.47	21.25	10.02	174.70	0.0490
Na	0.15	0.14	74.10	3.55	0.0008
Ga	0.03	0.01	67.31	0.37	0.0002
Mg	0.23	0.20	63.05	8.05	0.0016
P	3.60	2.56	8.78	112.26	0.0297
Au	18.12	2.02	9.87	231.72	0.1353
S	16.74	11.47	4.91	483.23	0.1348
Pd	5.10	1.05	23.18	58.91	0.0335
K	0.18	0.10	82.64	3.46	0.0014
Ca	6.29	3.45	13.26	101.87	0.0506

Fig. 9. Energy dispersive X-ray spectrum of the centre of a Ga-cut basal hook of a *Centrorhynchus globocaudatus* specimen showing considerably low levels of calcium and phosphorous compared to middle hooks (fig. 8), but markedly higher levels of sulphur (see bolded figures in table 5). Insert: SEM of a cross section of a basal proboscis hook.

cuts, as well as at the basal arch of hooks where tension and strength are paramount for hook function. The sulphur levels were very low throughout but relatively higher at the edge of hook tip cuts (table 4 and fig. 6). The chemical elements present in the hooks are typical for acanthocephalans (Heckmann *et al.*, 2007, 2012). Note the moderate outer layer (fig. 6) of the hook that relates to the sulphur content in the hook of *C. globocaudatus*, which is different than in other acanthocephalans. The high sulphur content shows up in the outer edge of X-ray scans of hooks (tables 4 and 5; Amin *et al.*, 2018). The hook centre in mid cuts has a different chemical profile than the cortical layer (table 4). The distribution of metals varied along the longitudinal axis of hooks on the proboscis, with apical and middle hooks having the highest levels of phosphorous and calcium but the lowest levels of sulphur compared to basal hooks (table 5 and figs 8, 9). The increased level of phosphorous (9.01% weight) in the developing embryo at the centre of eggs but not in its cortical layer (1.24) is noteworthy (table 6). Amin & Larsen (1989) found

high levels of phospholipids in the core and nucleus of ripe eggs but none in the unripe eggs or ovarian balls of *Neoechinorhynchus cylindratus* (Van Cleave, 1913) Van Cleave, 1919. Sheema (2018) reported intense acid phosphate activity in the eggs of *Echinorhynchus veli* George & Nadakal, 1978 in agreement with the histochemical observations of Amin & Larsen (1989), Crompton (1963) in *P. minutus* (Goeze, 1782) Lühe, 1911 and Cain (1970) in *M. hirudinaceus* (Pallas, 1781) Travassos, 1917. Sheema (2018) noted intense phosphatase activity in eggs associated with accelerated cellular metabolism. Anantaraman & Ravindranath (1976) observed that the protein in the wall of the acanthor of *Acanthosentis* sp. was rich in aromatic and sulphur-containing amino acids, which agrees with our observations in table 5.

X-ray scans (EDXA) provide insight into the hardened components – for example, calcium, sulphur and phosphorus – of acanthocephalan hooks. The EDXA appears to be species specific, as in fingerprints. For example, EDXA is shown to have

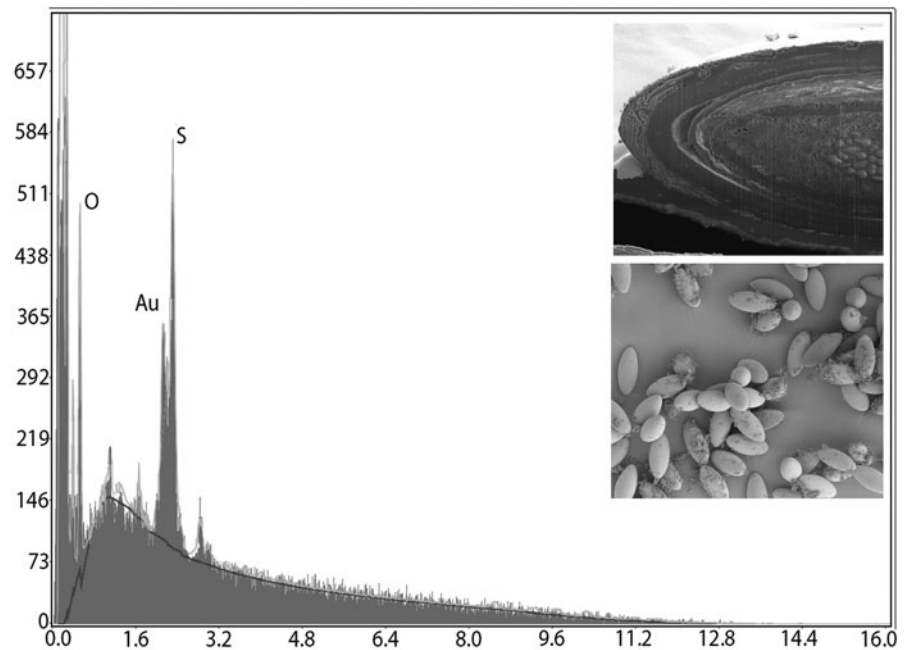


Fig. 10. Energy dispersive X-ray spectrum of the centre of the edge of a GA-cut egg of a *Centrorhynchus globocaudatus* female specimen showing a markedly high levels of sulphur (see bolded figures in [table 6](#)) and low levels of other metals tested. Insert: SEM of a part of Ga-cut egg; see [fig. 3f](#) for detail.

Element	Weight %	Atomic %	Error %	Net Int.	K Ratio
C	28.87	46.12	23.23	101.47	0.1287
N	15.98	21.89	26.70	32.74	0.0458
O	16.41	19.68	11.89	78.31	0.0538
Na	0.45	0.38	72.24	4.56	0.0026
Ga	2.43	0.67	23.98	13.85	0.0177
Mg	0.11	0.09	99.99	1.56	0.0007
P	1.24	0.77	24.81	15.45	0.0100
Au	16.98	1.65	9.53	86.84	0.1243
S	12.94	7.75	5.68	151.22	0.1033
Cl	0.02	0.01	99.99	0.19	0.0001
Pd	3.98	0.72	31.85	18.70	0.0261
K	0.11	0.06	99.99	0.88	0.0009
Ca	0.47	0.22	70.26	3.06	0.0037

significant diagnostic value in acanthocephalan systematics – for example, *Moniliformis cryptosaudi* Amin, Heckmann, Sharifdini & Albayati, 2019 was erected based primarily on its EDXA pattern (Amin *et al.*, 2019b). Our methodology for the detection of the chemical profile of hooks in the Acanthocephala has also been used in other parasitic groups including the Monogenea (Rubtsova *et al.*, 2018; Rubtsova & Heckmann, 2019) and Cestoda (Rubtsova & Heckmann, 2020). We also provide chemical and molecular data to explain and clarify our findings.

Molecular discussion

The results of phylogenetic analyses further support the description of the material described herein as *C. globocaudatus*. Indeed, present sequences unequivocally group with members of the same species published by García-Varela *et al.* (2020a) in the 18S phylogram. Unfortunately, no other sequences of this species are available to perform comparisons among different populations by *cox1* gene.

Although low bootstrap values are observed in most nodes of the SSU gene-based tree, due to low genetic signal, DNA sequence identity, determined according the alignment average distance under the *p*-distance model, yielded a value of 0.05 (95% identity). Therefore, alignment accuracy is, by far, high enough to build a reliable phylogenetic tree (Kumar & Filipski, 2006).

Actually, the SSU gene would be more adequate to address inter-generic or inter-familial phylogenetic relationships rather than interspecific ones, as is the case. Unfortunately, as already noted by Steinauer *et al.* (2019), the study of the relationships among centrorhynchid taxa based on molecular data is difficult due to the low number of sequences available – in particular, no SSU gene sequences are available for other genera of Centrorhynchidae. Thus, there is a great lack of information on the genus under study and any additional phylogeny that could be provided for *Centrorhynchus* can be valuable; this is especially true in the present case, in which a new geographical variant characterized by novel morphological aspects is described.

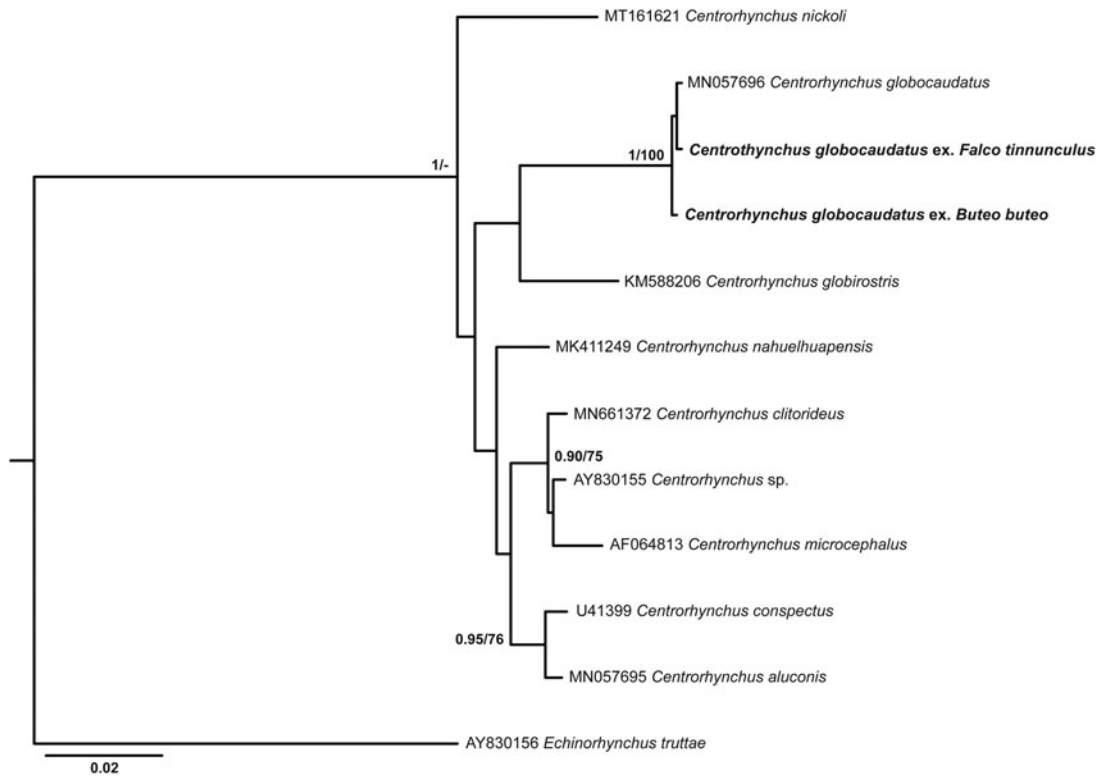


Fig. 11. BI phylogram reconstructed using two newly generated 18S rDNA sequences of *Centrorhynchus globocaudatus* and retrieved sequences from GenBank for Centrorhynchidae. Outgroup: *Echinorhynchus truttae*. Newly generated sequences are highlighted in bold. Nodal support from ML and BI analyses are indicated as BI/ML. Bootstrap values lower than 70 and posterior probability values lower than 0.9 are omitted. Scale bar indicates expected number of substitutions per site.

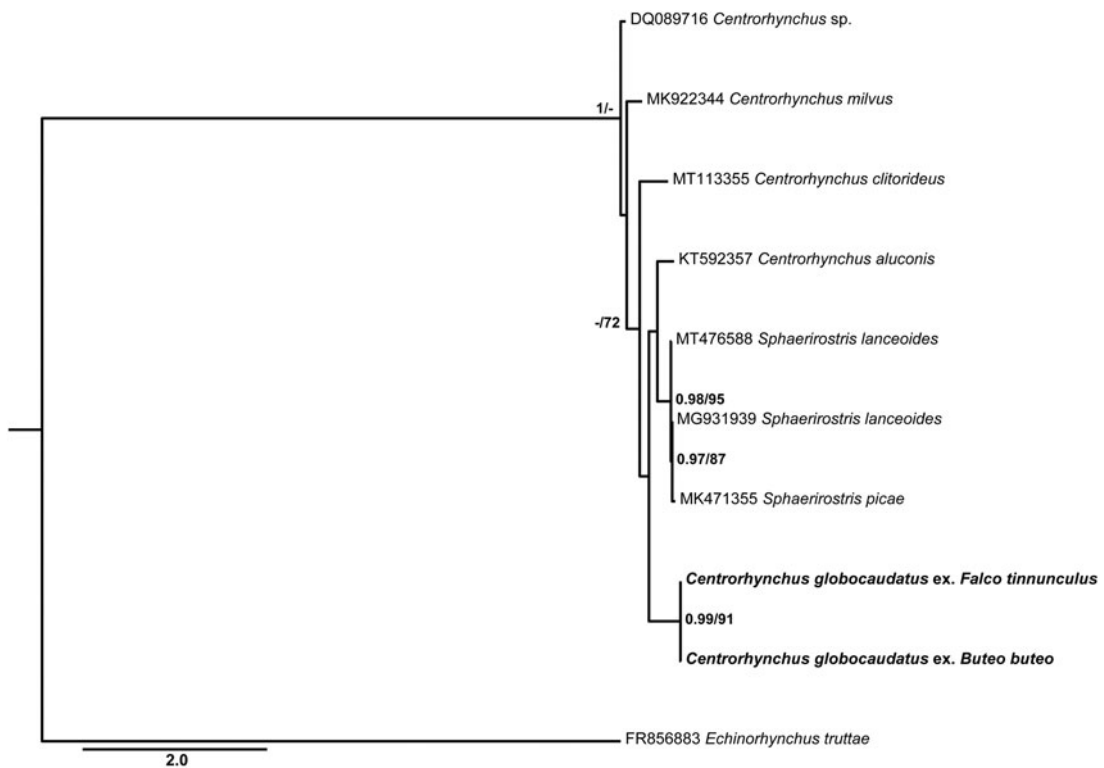


Fig. 12. ML phylogram reconstructed using two newly generated *cox1* sequences of *Centrorhynchus globocaudatus* and retrieved sequences from GenBank for Centrorhynchidae. Outgroup: *Echinorhynchus truttae*. Newly generated sequences are highlighted in bold. Nodal support from ML and BI analyses are indicated as BI/ML. Bootstrap values lower than 70 and posterior probability values lower than 0.9 are omitted. Scale bar indicates expected number of substitutions per site.

Table 7. Matrix of the pairwise 18S (left) and *cox1* (right) nucleotide genetic distances among *Centrorhynchus* and *Sphaerirostris* species.

	1	2	3	4	5	6	7	8	9	10		
1	<i>C. globocaudatus</i> MT993836		175	117	169	157	164	164	177	177	<i>C. milvus</i> MK922344	I
2	<i>C. globocaudatus</i> MT993837	0		171	167	174	163	161	172	171	<i>C. clitorideus</i> MT113355	H
3	<i>C. globocaudatus</i> MN057696	0	0		162	152	165	166	166	166	<i>Centrorhynchus</i> sp. DQ089716	G
4	<i>C. conspectus</i> U41399	25	25	25		124	11	30	163	162	<i>S. lanceoides</i> MT476588	F
5	<i>C. aluconis</i> MN057695	25	25	25	4		131	131	16	161	<i>C. aluconis</i> KT592357	E
6	<i>C. globirostris</i> KM588206	29	29	29	27	25		19	159	158	<i>S. lanceoides</i> MG931939	D
7	<i>Centrorhynchus</i> sp. AY830155	29	29	29	12	11	25		159	158	<i>S. picae</i> MK471355	C
8	<i>C. nahuelhuapensis</i> MK411249	31	31	31	14	14	25	13		1	<i>C. globocaudatus</i> MT992255	B
9	<i>C. microcephalus</i> AF064813	34	34	34	17	16	30	7	18		<i>C. globocaudatus</i> MT992256	A
10	<i>C. clitorideus</i> MN661372	30	30	30	13	12	26	3	14	8		
11	<i>C. nickoli</i> MT161621	39	39	39	29	27	30	23	27	28	24	
		I	H	G	F	E	D	C	B	A		

Outcomes of phylogenetic analyses based on mtDNA data (Muhammad *et al.*, 2020) suggest that *Sphaerostris* is a sister group of *Centrorhynchus aluconis*, conforming a sub-clade within *Centrorhynchus*, which would, therefore, be a paraphyletic taxon. Our results seem to agree with this suggestion; however, the weak bootstrap support and the nucleotide differences associated to these relationships in phylogenetic analyses hamper its confirmation. In addition, the genera *Centrorhynchus* and *Sphaerostris* have been well differentiated based on morphology (see Table 1 in Amin & Canaris, 1997). Specifically, one of the clearest diagnostic features allowing discrimination between both genera, the lacunar system pattern, is recognized as one of the most important taxonomic criteria in the classification of the Acanthocephala at the generic and higher levels (Amin & Canaris, 1997). The short spindle-shaped trunk and short globular anterior proboscis in *Sphaerostris* clearly distinguish it from *Centrorhynchus*, with a long cylindrical trunk and long cylindrical anterior proboscis, among other features.

The two *cox1* available sequences of *Sphaerostris lanceoides* were obtained from cystacanths present in amphibians and ardeid birds (i.e. *Ardeola grayii*), respectively (Kang & Li, 2018; Muhammad *et al.*, 2020), and the only *cox1* available sequence of *Sphaerostris picae* was obtained from adults infecting the corvid *Dendrocitta vagabunda* (see Muhammad *et al.*, 2019). Indeed, while *Sphaerostris* mostly infects passerine birds, *Centrorhynchus* mainly infects birds of prey instead. Therefore, ecological associations between parasites and their hosts further support morphological studies in marking a differentiation between these two centrorhynchid genera. Interestingly, a study based on 18S DNA gene analysis revealed the relatively close relation of *S. picae* with *Plagiorhynchus cylindraceus* (Goeze, 1782) (Plagiorhynchidae), even more than with other species of the genus *Centrorhynchus* (Radwan, 2012). However, 18S and 28S sequences obtained by Radwan (2012) were too short, from our point of view, to yield fully reliable phylogenetic affinities (361 and 281 bp); thus, they were not included in present analyses. Apart from these ones, no 18S sequences have been made available for *S. picae* or other *Sphaerostris* members up to date, which would have helped better elucidate their phylogenetic relationship to *Centrorhynchus* representatives.

In conclusion, phylogenetic relationships within the Centrorhynchidae remain unsolved. It becomes clear that more *Sphaerostris* sequences obtained from well-characterized adult and properly identified specimens, as well as genetic data of the third genus within the family, *Neolacunisoma*, are needed in order to clarify phylogenetic associations within the Centrorhynchidae.

Acknowledgements. We are indebted to Dr Bahram S. Dezfuli, University of Ferrara, Italy, for meticulous coordination of the Italian operation run by S. Rubini at the Experimental Zooprophyllactic Institute of Ferrara, where recovery of parasites took place with the US researchers. We thank Dr Nataliya Rubtsova (Parasitology Center, Inc.) and Madison Laurence, Bean Museum (Brigham Young University), Provo, Utah, for their expert help in the preparation and organization of plates and figures, and Michael Standing, Electron Optics Laboratory (Brigham Young University), for his technical help and expertise.

Financial support. This project was supported by an institutional grant from the Biology Department, Brigham Young University, Provo, Utah, and the Parasitology Center, Inc., Scottsdale, Arizona.

Conflicts of interest. None.

Ethical standards. The authors declare that they have observed all applicable ethical standards.

References

- Amin OM (2013) Classification of the Acanthocephala. *Folia Parasitologica* **60** (4), 273–305.
- Amin OM and Canaris A (1997) Description of *Neolacunisoma geraldsmithi* gen. n., sp. n., (Acanthocephala: Centrorhynchidae) from South African shorebirds. *Journal of Helminthological Society of Washington* **64**, 275–280.
- Amin OM and Dailey MD (1998) Description of *Mediorhynchus papillosus* (Acanthocephala: Gigantorhynchidae) from a Colorado, U.S.A., population, with a discussion of morphology and geographical variability. *Journal of the Helminthological Society of Washington* **65**, 189–200.
- Amin OM and Larsen D (1989) Acanthocephala from lake fishes in Wisconsin: a biochemical profile of *Neoechinorhynchus cylindricus* (Neoechinorhynchidae). *Transactions of the American Microscopical Society* **108**, 309–315.
- Amin OM, Heckmann RA, Radwan NA, Mantuano JS and Alcivar MAZ (2009) Redescription of *Rhadinorhynchus ornatus* (Acanthocephala: Rhadinorhynchidae) from skipjack tuna, *Katsuwonus pelamis*, collected in the Pacific Ocean off South America, with special reference to new morphological features. *Journal of Parasitology* **95**, 656–664.
- Amin OM, Heckmann RA, Halajian A and El-Naggar AM (2011) The morphology of an unique population of *Corynosoma strumosum* (Acanthocephala, Polymorphidae) from the Caspian seal, *Pusa caspica*, in the land-locked Caspian Sea using SEM, with special notes on histopathology. *Acta Parasitologica* **56**, 438–445.
- Amin OM, Heckmann RA, Wilson E, Keele B and Khan A (2015) The description of *Centrorhynchus globirostris* n. sp. (Acanthocephala: Centrorhynchidae) from the pheasant crow, *Centropus sinensis* (Stephens) in Pakistan, with gene sequence analysis and emendation of the family diagnosis. *Parasitology Research* **114**, 2291–2299.
- Amin OM, Heckmann RA and Bannai M (2018) *Cavisoma magnum* (Cavisomidae), a unique Pacific acanthocephalan redescribed from an unusual host, *Mugil cephalus* (Mugilidae), in the Arabian Gulf, with notes on histopathology and metal analysis. *Parasite* **25**, 5.
- Amin OM, Heckmann RA, Dallarés S, Constenla M and Ha NV (2019a) Morphological and molecular description of *Rhadinorhynchus laterospinosus* Amin, Heckmann & Ha, 2011 (Acanthocephala, Rhadinorhynchidae) from marine fish off the Pacific coast of Vietnam. *Parasite* **26**, 14.
- Amin OM, Heckmann RA, Sharifdini M and Albayati NY (2019b) *Moniliformis cryptosaudi* n. sp., (Acanthocephala: Moniliformidae) from the long-eared hedgehog *Hemiechinus auratus* (Gmelin) (Erinaceidae) in Iraq; a case of incipient cryptic speciation related to *M. Saudi* in Saudi Arabia. *Acta Parasitologica* **64**, 195–204.
- Anantaraman S and Ravindranath MN (1976) Histochemical characteristics of the egg envelopes of *Acanthosentis oligospinus* (Acanthocephala). *Zeitschrift für Parasitenkunde* **48**, 227–238.
- Bergman G (1961) The food of birds of prey and owls in Fenno-Scandia. *British Birds* **54**, 307–320.
- Bhattacharya SB (2000) *Fauna of Tripura*. Zoological Survey of India, State Fauna Series 7, Part 4, 1–355.
- Bhattacharya SB (2006) *Handbook on Indian Acanthocephala*. Kolkata, Zoological Survey of India, 225 pp.
- Bhattacharya SB (2007) *Handbook on Indian Acanthocephala*. Kolkata, Zoological Survey of India. 255 pp.
- Byram JE and Fisher FM Jr (1973) The absorptive surface of *Moniliformis dubius* (Acanthocephala). 1. Fine structure. *Tissue Cell* **5**, 553–579.
- Cain GD (1970) Collagen from the giant acanthocephalan *Macracanthorhynchus hirudinaceus*. *Archives of Biochemistry and Biophysics* **141**, 264–270.
- Cramp S and Brooks DJ (1992) *Handbook of the birds of Europe, the Middle East and North Africa. The birds of the western Palearctic, vol. 2*. Oxford, Oxford University Press.
- Crompton DWT (1963) Morphological and histochemical observations on *Polymorphus minutus* (Goeze, 1782) with special reference to the body wall. *Parasitology* **53**, 663–685.
- Darriba D, Taboada GL, Doallo R and Posada D (2012) jModelTest 2: more models, new heuristics and parallel computing. *Nature Methods* **9**, 772.

- Dereeper A, Guignon V, Blanc G, et al. (2008) Phylogeny.fr: robust phylogenetic analysis for the non-specialist. *Nucleic Acids Research* **36**(web server issue), W465–W469.
- Dezfuli BS, Rubini S, DePasquale JA and Pironi F (2020) Ultrastructure of male *Centrorhynchus globocaudatus* (Acanthocephala) cement apparatus and function of cement gland secretion. *Journal of Helminthology* **94**, e161, 1–7.
- Dimitrova ZM and Gibson DI (2005) Some species of *Centrorhynchus* Luhe, 1911 (Acanthocephala: Centrorhynchidae) from the collection of the Natural History Museum, London. *Systematic Parasitology* **62**, 117–134.
- Dimitrova ZM, Murai E and Gerogiev BB (1995) Some species of the family Centrorhynchidae Van Cleave, 1916 (Acanthocephala) from Hungarian birds. *Parasitologia Hungarica* **28**, 89–99.
- Dimitrova ZM, Gerogiev BB and Genov T (1997) Acanthocephalans of the family Centrorhynchidae (Palaeacanthocephala) from Bulgaria. *Folia Parasitologica* **44**, 224–232.
- Dipineto L, Borelli L, Pepe P, Fioretti A, Caputo V, Cringoli G and Rinaldi L (2013) Synanthropic birds and parasites. *Avian Diseases* **57**, 756–758.
- Florescu BI and Ienistea MA (1984) Aperçu sur les acanthocephales de Roumanie (Acanthocephala). *Travaux du Museum d'Histoire Naturelle Grigore Antipa* **25**, 7–45.
- García-Varela M and Nadler SA (2005) Phylogenetic relationships of Palaeacanthocephala (Acanthocephala) inferred from SSU and LSU rDNA gene sequences. *Journal of Parasitology* **91**(6), 1401–1409.
- García-Varela M, Pérez-Ponce de León G, de la Torre P, Cummings MP, Sarma SSS and Lacleste JP (2000) Phylogenetic relationships of Acanthocephala based on analysis of 18S ribosomal RNA gene sequences. *Journal of Molecular Evolution* **50**, 532–540.
- García-Varela M, Park J-K, Hernández-Orts JS and Pinacho-Pinacho CD (2020a) Morphological and molecular data on a new species of *Plagiorhynchus* Lühe, 1911 (Acanthocephala: Plagiorhynchidae) from the long-billed curlew (*Numenius americanus*) from northern Mexico. *Journal of Helminthology* **94**, e61.
- García-Varela M, Andrade-Gómez L, López-Caballero J, Mendoza-Garfias B, Oceguera-Figueroa A and Mata-López R (2020b) Morphological and molecular data reveal a new species of *Lueheia* (Acanthocephala: Plagiorhynchidae) from *Turdus migratorius* (Turdidae) in central Mexico and its phylogenetic implications within the family. *Parasitology Research*. **19**(10), 1–11. doi:10.1007/s00436-020-06748-7.
- Gazi M, Kim J, García-Varela M, Park C, Littlewood DTJ and Park JK (2016) Mitogenomic phylogeny of Acanthocephala reveals novel Class relationships. *Zoologica Scripta* **45**(4), 437–454.
- Guindon S, Dufayard JF, Lefort V, Anisimova M, Hordijk W and Gascuel O (2010) New algorithms and methods to estimate maximum-likelihood phylogenies: assessing the performance of PhyML 3.0. *Systematic Biology* **59**(3), 307–321.
- Gupta NK and Gupta K (1972) Observations on genus *Centrorhynchus* Luhe, 1911 (Acanthocephala: Gigantorhynchidea). *Research Bulletin of the Panjab University* **23**, 1–12.
- Heckmann RA, Amin OM and Standing MD (2007) Chemical analysis of metals in Acanthocephalans using energy dispersive X-ray analysis (EDXA, XEDS) in conjunction with a scanning electron microscope (SEM). *Comparative Parasitology* **74**, 388–391.
- Heckmann RA, Amin OM, Radwan NAE, Standing MD, Eggett DL and El Nagggar AM (2012) Fine structure and energy dispersive X-ray analysis (EDXA) of the proboscis hooks of *Radinorynchus ornatus*, Van Cleave 1918 (Radinorynchidae: Acanthocephala). *Scientia Parasitologica* **13**, 37–43.
- Heckmann RA, Amin OM and El-Nagggar AM (2013) Micropores of Acanthocephala, a scanning electron microscopy study. *Scientia Parasitologica* **14**, 105–113.
- Hoklova IG (1986) *The acanthocephalan fauna of terrestrial vertebrates of SSSR*. Moscow, Russia, Nauka. 276 pp.
- Huelsbeck JP, Ronquist F, Nielsen R and Bollback JP (2001) Bayesian inference of phylogeny and its impact on evolutionary biology. *Science* **294**, 2310–2314.
- Kang J and Li L (2018) First report on cystacanths of *Sphaeroirostris lanceoides* (Petrochenko, 1949) (Acanthocephala: Centrorhynchidae) from the Asiatic toad *Bufo gargarizans* Cantor (Amphibia: Anura) in China. *Systematics Parasitology* **95**, 447–454.
- Komorová P, Špakulová M, Hurníková Z and Uhrin M (2015) Acanthocephalans of the genus *Centrorhynchus* (Palaeacanthocephala: Centrorhynchidae) of birds of prey (Falconiformes) and owls (Strigiformes) in Slovakia. *Parasitology Research* **114**(6), 2273–2278.
- Kumar S and Filipski A (2006) Multiple sequence alignment: in pursuit of homologous DNA positions. *Genome Research* **17**, 127–135.
- Lee RE (1992) *Scanning electron microscopy and x-ray microanalysis*. Englewood Cliffs, New Jersey, Prentice Hall, p. 458.
- Lisitsyna OI (2019) *Fauna of Ukraine*, Vol. 31. Acanthocephala. Naukova dumka, Kyiv, 1–223 (in Russian).
- Lisitsyna OI and Greben OB (2015) Acanthocephalans of the genus *Centrorhynchus* (Palaeacanthocephala, Centrorhynchidae) from birds of Ukraine with the description of a new species. *Vestnik Zoologii* **49**, 195–210.
- Meyer A (1932) *Acanthocephala*. Dr. H.G. Bronns, Klassen und Ordnungen des Tier-Reichs, Leipzig, Bd. 4, 2 Abt., 2 Buch, I Lief.: 1–332.
- Miller MA, Pfeiffer W and Schwartz T (2010) Creating the CIPRES Science Gateway for inference of large phylogenetic trees. pp. 1–8 in *Proceedings of the Gateway Computing Environments Workshop (GCE)*, 14 November 2010, New Orleans, Los Angeles.
- Muhammad N, Ma J, Khan MS, Li L, Zhao Q, Ahmad MS and Zhu XQ (2019) Characterization of the complete mitochondrial genome of *Sphaeroirostris picae* (Rudolphi, 1819) (Acanthocephala: Centrorhynchidae), representative of the genus *Sphaeroirostris*. *Parasitology Research* **118**, 2213–2221.
- Muhammad N, Suleman S, Saleem Ahmad M, Li L, Zhao Q, Ullah H, Zhu X-Q and Ma J (2020) Mitochondrial DNA dataset suggest that the genus *Sphaeroirostris* Golvan, 1956 is a synonym of the genus *Centrorhynchus* Lühe, 1911. *Parasitology* **147**, 1149–1157.
- Naidu K (2012) *Fauna of India and Adjacent Countries. Acanthocephala*. Zoological Survey of India. Kolkata. 638 pp.
- Nelson DR and Ward HL (1966) Acanthocephala from hedgehogs in Egypt. *Journal of the Tennessee Academy of Science* **41**, 101–105.
- Petrochenko VI (1950) Notes sur les acanthocephales des oiseaux de la Kirghizie du Sud. *Trudy Gelminthologicheskoi Laboratorii, Akademii Nauk S.S.S.R.* **4**, 100–105 (in Russian).
- Petrochenko VI (1958) *Acanthocephala of domestic and wild animals*. Vol. 2. Moscow, Isdatel'stv Akademii Nauk SSSR, Moscow.
- Radwan NA (2012) Phylogenetic analysis of *Sphaeroirostris picae* (Acanthocephala: Centrorhynchidae) based on large and small subunit ribosomal DNA gene. *International Journal of Parasitology Research* **4**(2), 106–110.
- Rainboth WJ (1996) *Fishes of the Cambodian Mekong*. FAO species identification field guide for fisheries purpose. Rome, FAO. 265 pp.
- Ronquist F, Teslenko M, Van Dermark P, Ayres DL, Darling A, Höhna S, Larget B, Liu L, Suchard MA and Huelsenbeck JP (2012) MrBayes 3.2: efficient Bayesian phylogenetic inference and model choice across a large model space. *Systematic Biology* **61**, 539.
- Rubtsova NY and Heckmann RA (2019) Structure and morphometrics of *Ancyrocephalus paradoxus* (Monogenea: Ancyrocephalidae) from *Sander lucioperca* (Percidae) in Czechia. *Helminthologia* **56**(1), 11–21.
- Rubtsova NY and Heckmann RA (2020) Morphological features and structural analysis of plerocercoids of *Spirometra erinacieuropaei* (Cestoda: Diphyllbothriidae) from European pine marten, *Martes martes* (Mammalia: Mustelidae) in Ukraine. *Comparative Parasitology* **87**(1), 109–117.
- Rubtsova NY, Heckmann RA, Smit WS, Luus-Powell WJ, Halajian A and Roux F (2018) Morphological studies of developmental stages of *Oculotrema hippopotami* (Monogenea: Polystomatidae) infecting the eye of *Hippopotamus amphibius* (Mammalia: Hippopotamidae) using SEM and EDXA with notes on histopathology. *Korean Journal of Parasitology* **56**(5), 463–475.
- Rudolphi KA (1802) Fortsetzung der Beobachtungen über die Eingeweidewürmer. *Wiedmann's Archiv Zoologie Zootomie, Braunschweig* **2**(2), 1–67.

- Santoro M, Tripepi M, Kinsella JM, Panebianco A and Mattiucci S** (2010) Helminth infestation in birds of prey (Accipitriformes and Falconiformes) in Southern Italy. *The Veterinary Journal* **186**(1), 119–122.
- Sheema SH** (2018) Histochemical studies on acanthocephalan parasite, *Echinorhynchus veli* infecting the fish *Synaptura orientalis* (BI & Sch, 1801). *International Journal of Scientific Research and Reviews* **7**(12), 1–25.
- Steinauer M, Flores VR and Rauque CA** (2019) *Centrorhynchus nahuelhualpensis* n. sp. (Acanthocephala: Centrorhynchidae) from rufous-legged owl (*Strix rufipes* King) in Patagonia. *Journal of Helminthology* **94**, 1–7.
- Tamura K, Stecher G and Peterson D** (2013) MEGA6: molecular evolutionary genetics analysis version 6.0. *Molecular Biology and Evolution* **30**, 2725–2729.
- Torres P and Puga S** (1966) Occurrence of cystacanths of *Centrorhynchus* sp. (Acanthocephala: Centrorhynchidae) in toads of the genus *Eupsophus* in Chile. *Memorias do Instituto Oswaldo Cruz* **91**(6), 717–719. Rio de Janeiro. Nov./Dec.: 1–3 (online version).
- Viitala J, Korpimäki E, Palokangas P and Koivula M** (1995) Attraction of kestrels to vole scent marks visible in ultraviolet light. *Nature* **373**(6513), 425–427.
- Ward HL** (1964) Acanthocephala from the little owl, *Athene noctua*, in Egypt. *Journal of the Tennessee Academy of Science* **39**(3), 83–85.
- Whitfield PJ** (1979) *The biology of parasitism: an introduction to the study of associating organisms*. Baltimore, Maryland, University Park Press. p. 277.
- Wright RD and Lumsden RD** (1969) Ultrastructure of the tegumentary pore-canal system of the acanthocephalan *Moniliformis dubius*. *Journal of Parasitology* **55**, 993–1003.
- Yamaguti S** (1963) *Acanthocephala*. Systema Helminthum. New York, London, Wiley Intersci., **5**, 1–423.
- Zeder JGH** (1800) Erster Nachtrag zur Naturgeschichte der Eingeweidewürmer von Joh. Aug. Ephr. Goeze. Mit Zusätzen und Anmerkungen. *Leipzig* **4**, 101–143.
- Zhao Q, Muhammad N, Chen H-X, Ma J and Suleman LL** (2020) Morphological and genetic characterization of *Centrorhynchus clitorideus* (Meyer, 1931) (Acanthocephala: Centrorhynchidae) from the little owl *Athene noctua* (Scopoli) (Strigiformes: Strigidae) in Pakistan. *Systematic Parasitology* **97**, 517–528.